

# Simulation Study of Aspects of the Classical Hydrogen Atom Interacting with Electromagnetic Radiation: Circular Orbits

Daniel C. Cole and Yi Zou

*Dept. of Manufacturing Engineering, 15 St. Mary's Street,  
Boston University, Boston, Massachusetts 02446*

(Dated: July 13, 2002)

## Abstract

The present study examines the behavior of a classical charged point particle orbiting an infinitely massive and oppositely charged nucleus, while acted upon by circularly polarized electromagnetic plane waves. This system is intended to represent a classical model of a hydrogen atom interacting with radiation. Despite the simplicity of the system, very nonlinear behavior result, making a numerical study of the system nearly essential. The results should be of interest to researchers studying the classical behavior of Rydberg-like atoms. The numerical results naturally suggest a number of experiments that could be done involving the novel control of chemical reactions and of excited atomic states. Moreover, and perhaps more immediately, the present article has close ties and implications regarding the behavior of the classical hydrogen atomic model within the domain of the theory called stochastic electrodynamics.

## I. INTRODUCTION

Here we will examine the behavior of a classical physical model of hydrogen consisting of a  $-e$  charged point particle orbiting an infinitely massive nucleus, consisting of a  $+e$  point charge. The system is in many ways certainly very simple, but, as is well known to researchers pursuing the simulation of planetary orbits over long time periods, the subtle aspects of its very nonlinear behavior is far from trivial. Here we will examine in depth the behavior of the orbiting  $-e$  charge in near circular orbit about the  $+e$  charge, while under the influence of a selected set of electromagnetic plane waves. We will assume that the trajectory of the  $-e$  charge is described by the classical Lorentz-Dirac (LD) equation.

Why are we interested in such a system? There are three main reasons. First, such a system is often considered for understanding the behavior of atoms placed into excited Rydberg states, so that the outer electron makes a relatively large orbit from the nucleus and other electrons, which can then be approximated as a hydrogen-like atom. In relatively recent years, a number of researchers have shown considerable interest in studying Rydberg-like atoms, with many of their advances involving fascinating experimental results. “Even today, research into perturbative long-range interactions continues to push into new territory, driven largely by the experimental capabilities of Rydberg state spectroscopy to detect effects of extremely weak interactions. ... The astonishing precision of high resolution Rydberg state spectroscopy provides a revealing probe of small and large perturbations.” [1] Complex, subtle, and non-intuitive behavior of these simple systems is being revealed by a wide variety of experimental probes, including the now heavily-examined splitting of Rydberg atomic energy levels due to applied electric and magnetic fields [2], the ionization of electrons in Rydberg states due to applied circularly and elliptically polarized microwave fields [3], investigations of stabilization of Rydberg states in intense laser fields [4], more recent investigations of fast and slow electromagnetic pulsing of Rydberg atoms [5],[6], a probing of anisotropic induced electric dipole ionic behavior due to a relatively slow Rydberg electron motion behavior [1], and recent ionization analysis for full 3D Rydberg atoms [7]. Much of our present physical insight into these experimental results comes from a classical physical examination of the situation [8],[1],[5],[9], which has since been contrasted in numerous studies with quantum mechanical predictions [8],[5]. The present study should be of aid in such considerations, not so much with regard to ionization, but rather with

regard to stabilization in intense electromagnetic fields [4],[10].

These investigations clearly illustrate a wide range of abilities for controlling various atomic system behaviors. Indeed, the richness of the phenomena being experimentally revealed, by applying fairly simple time varying electromagnetic fields on equally very simple atomic systems, is really quite staggering. By varying frequencies and amplitudes of applied electromagnetic radiation, and possibly adding in fast “kicked” pulses, the ionization rates and even stabilization domains are being profoundly affected. Without doubt, atoms more complicated than hydrogen and Rydberg atoms, also display extremely rich phenomena, when electromagnetic laser and other electromagnetic sources of radiation are applied to probe the dynamics of inner shell electron behavior.

Most physicist’s intuition of what should take place for atoms irradiated with electromagnetic radiation, undoubtedly lie with the early classic experiments of the photoelectric effect, where if the frequency of the radiation is below some threshold value, then no ionization takes places, regardless of the intensity of the radiation. Moreover, the maximum kinetic energy of ejected electrons from metals irradiated with light, increase linearly in proportion to the frequency of the light beyond this minimum frequency threshold value. Yet, the phenomena being revealed in the more recent experiments discussed in Refs. [1]-[10], go well beyond these early photoelectric effects that puzzled physicists so deeply around the 1900 time period. Advanced radiation sources, particularly involving the laser, are now enabling detailed control of atomic systems that were nearly impossible to anticipate in the early 1900s. Yet, these more recent experiments still only involve relatively simple atomic systems with relatively simple radiation controls. Undoubtedly the richness of phenomena for more complex systems, will be deep. The likely reason scientists have concentrated on these relatively simple atomic situations, is that the phenomena are quite rich, but the situation is analyzable by present techniques and ideas, including semiclassical approaches.

Our second main reason for studying the classical atomic system described here, is the following. By controlling the behavior of atomic systems with electromagnetic radiation, in ways previously either not considered and/or simply not examined in any detail, a plethora of new applications become possible. Chemical reactions should be controllable to perhaps great extents by appropriately applied radiation and electromagnetic fields. Instrumentations and fabrication techniques, such as in etching, deposition, ion implantation, and sputtering, might well be controllable in far greater degree than presently available, if the

right ideas can be arrived at for making use of applied radiation signals, as a function of time, while such interactions are taking place. Indeed, to some extent these ideas are already implemented, such as in rapid laser annealing in semiconductor technology, plasma controlled etching techniques, isotope separation methods, and improved ion source generators. However, there are undoubtedly far more instances of control yet to be developed, provided scientists and technologists can make use of the right ideas. To support such speculations, we note that a number of patents have been issued in the past 25 years or so, that pertain to manipulating Rydberg atomic states for various application purposes (see, for example, Refs. [11],[12],[13],[14],[15]).

The third main reason for our present study, which in truth is our main motivation, has to do with pushing further on the ideas of stochastic electrodynamics (SED) [16],[17],[18],[19]. SED is a classical theory of electrodynamics that involves the use of Maxwell's equations for describing the electromagnetic fields, combined with the relativistic version of Newton's second law of motion for describing the trajectory of classical electrodynamic particles, and supplemented by the idea that most experimental tests necessarily involve the critically important presence of incident radiation fields influencing the particle trajectories, present even at a temperature  $T = 0$  [18],[20]. The key physical ideas and important initial calculations were introduced quite clearly by Marshall [21],[22] and Boyer [23],[24] in the 1960s, although a number of other researchers certainly had earlier ideas that tie in with this work in various ways, as nicely described in Ref. [17] (see Ref. [25]).

The present status of SED seems to be that many scientists find the SED ideas of some interest, for a number of reasons [17],[19], but not promising in terms of much deeper agreement with nature than what has already been established. Consequently, SED seems to have been abandoned by most researchers, and there has not been much progress in recent years to offset any of the original core criticisms. A quick, but reasonably accurate summary of the status might be the following: SED works well for linear systems, such as for a fairly wide variety of systems of electric dipole simple harmonic oscillators (SHOs) [16], as well as for electromagnetic fields interacting linearly with macroscopic media boundaries, like conducting walls and dielectric plates, that occur in most experiments to date with Casimir and van der Waals forces [26],[27]. In addition, there are a wide range of quantum optical experiments that have interesting explanations from within the SED related branch called stochastic optics, as has largely been led by Marshall, Santos, and their collaborators, as

reviewed in Ref. [17]. Other SED-related physics areas of interest also exist, such as having to do with quantum cavity electrodynamics [28],[26] and the thermal effects of acceleration of simple electrodynamic systems through the vacuum [29],[30],[31],[32], as well as a host of other SED articles on topics as diverse as diamagnetism, paramagnetism, blackbody radiation, and excited states (see Sec. 1 in Ref. [16] for a quick summary of this work). However, aside from these often surprising insights between the differences of classical and quantum physics [17], the full direction of SED as originally envisioned [18],[33], has to date not been realized.

Indeed, for electrodynamic system governed by nonlinear equations of motion, there has in general not been agreement between SED and quantum electrodynamics (QED). Reference [16] provides a concise summary of the status of these discrepancies, with major work here being provided by [34],[35],[36],[37],[38],[39],[40],[41]. The main consensus by most researchers is that SED has shown some interesting connections between classical and quantum physics, by including a classical concept involving the single idea of not imposing that motion and fields must equal zero at temperature  $T = 0$ ; indeed, strong arguments, based on equilibrium ideas between charges and fields provide incentive for why motion and fields should not equal zero at  $T = 0$  [20],[42]. However, most researchers seem to have concluded that this idea is not sufficient to bridge the gap for classical physical ideas to adequately describe nature. Indeed, there largely seems to be only two published arguments, not yet disproved [43],[44], that still provide hope that the original views of SED may yet be successful, if the theory is limited to strictly physical systems that really occur in nature. For atomic physics, this means full electrodynamic systems based on Maxwell's equations, without ad hoc considerations of nonlinear oscillator systems that in reality do not exist in full detail for atomic systems.

Returning to the thrust of the present article, we are examining a simple electrodynamic system, namely, a classical model of hydrogen. Other than the practical aspects of simply investigating a Rydberg atom, by solving this Keplerian classical system for a large number of orbits, and thereby contributing to the literature on understanding such a system classically, we also want to return to some of the original ideas motivating SED and examine this simple system as carefully as possible. However, the present work can certainly not claim to make too close a connection to SED, as we will not include classical electromagnetic zero-point (ZP) radiation in our present treatment. One of us some time ago attacked

this system with a rough, but very computationally intensive, description of the stochastic nature of ZP electromagnetic radiation. The problem is clearly a difficult one, due to the inherent difficulty of representing the stochastic electromagnetic fields adequately via simulation methods, without becoming too computationally intensive, but at the same time not leaving out key, important effects. Although interesting results have been found, clear directions are far from being established. Nevertheless, other insights will be discussed here, that show some of the richness of the nonlinear aspects of this simplest of atomic systems. Our hope is that some of the ideas suggested in the present article, plus other planned work, will help to improve on this rough description, without incurring impossibly computational situations due to the near infinite frequency range that is presumed to be present.

As we believe first described, Boyer in Ref. [18] discussed qualitatively how stability for a hydrogen atom might arise if the SED basic theoretical idea is correct. If we consider the atom in equilibrium with radiation at absolute zero temperature, then when the electron is far from the proton, the period of its orbit is large, so the electron should tend to interact most strongly with frequencies in the ZP radiation spectrum corresponding with this large period (*i.e.*, small frequency). The energy of the ZP radiation in the small frequency region is not enough to offset the energy that will be lost, on average, due to radiation reaction. Hence, on average, the electron should tend to spiral in toward the nucleus. As it spirals in, the period (frequency) of its orbit will decrease (increase), thereby making the electron interact more strongly with ZP radiation in a higher frequency regime. The average energy of ZP radiation, per frequency interval, increases as the frequency increases. Hence, on average, as the electron spirals in toward the nucleus, the ZP radiation will tend to impart energy to the electron, tending to make it start spiraling back out. The SED picture is then one of stochastic fluctuation, where the electron tends to spiral in and out, in just such a way as to fulfill the probability density distribution predicted by the ground state solution of Schrödinger's equation. The analysis of Ref. [18] shows that the average radius for this scenario is indeed roughly given by the Bohr radius of  $a_B = \hbar^2/me^2$ .

In the present article, Sec. II will be devoted to discussing the equation of motion of the orbiting electron, and its numerical solution. Section III will then provide a range of numerical results, starting from the numerical demonstration of the classical atomic collapse problem due to radiation reaction, followed by a discussion and demonstration on how the application of carefully selected applied radiation on the spiraling electron can stabilize

the orbit. Sections IV and V then turn to less obvious situations that reveal interesting nonlinear behavior that seem difficult to anticipate for this otherwise simple system. As will be shown, as the amplitude of the applied radiation is increased, stability still results for the orbiting electron, although it continuously spirals in and out toward the nucleus, within a small range. We then show numerical experiments for what happens if an electron is allowed to spiral in from a large radius toward the nucleus, when an intermediate resonant plane wave is present. As will be shown, the electron reacts strongly as the orbiting period of the electron crosses the frequency domain of the applied radiation. Section VI then ends with some concluding remarks and comments on where we expect this work to continue.

## II. EQUATION OF MOTION

The equation of motion for the  $-e$  charged classical electron, orbiting about the classical infinitely massive  $+e$  charge at the nucleus, is assumed here to be the Lorentz-Dirac equation of motion [45],[46],[47]:

$$m \frac{d^2 z^\mu}{d\tau^2} = \frac{2e^2}{3c^3} \left[ \frac{d^3 z^\mu}{d\tau^3} - \frac{1}{c^2} \left( \frac{d^2 z^\lambda}{d\tau^2} \frac{d^2 z_\lambda}{d\tau^2} \right) \frac{dz^\mu}{d\tau} \right] + F^\mu \quad , \quad (1)$$

where  $\tau$  is the proper time, and  $F^\mu$  is the four-force representing the sum of the effects due to the binding force of the nucleus, plus any other applied forces. Rewriting this in terms of three-vector notation [see Eqs. (5.25)-(5.27) in Ref. [48]], with the proper time expressed in terms of the coordinate time, with  $\gamma d\tau = dt$ ,  $\dot{\mathbf{z}} \equiv \frac{d\mathbf{z}}{dt}$ ,  $\ddot{\mathbf{z}} \equiv \frac{d^2\mathbf{z}}{dt^2}$ , and with  $\gamma \equiv [1 - (\dot{\mathbf{z}}/c)^2]^{-1/2}$ , then

$$\frac{d}{dt} (\gamma m \dot{\mathbf{z}}) = -\frac{e^2 \mathbf{z}}{|\mathbf{z}|^3} + \mathbf{R}_{\text{reac}} + (-e) \left\{ \mathbf{E}[\mathbf{z}(t), t] + \frac{\dot{\mathbf{z}}}{c} \times \mathbf{B}[\mathbf{z}(t), t] \right\} \quad , \quad (2)$$

where

$$\mathbf{R}_{\text{reac}} = \frac{2e^2}{3c^3} \left\{ \frac{d}{dt} \left[ \gamma^2 \ddot{\mathbf{z}} + \gamma^4 \left( \frac{\dot{\mathbf{z}}}{c} \cdot \ddot{\mathbf{z}} \right) \frac{\dot{\mathbf{z}}}{c} \right] - \frac{1}{c} \left[ \gamma^4 \ddot{\mathbf{z}}^2 + \gamma^6 \left( \frac{\dot{\mathbf{z}}}{c} \cdot \ddot{\mathbf{z}} \right)^2 \right] \frac{\dot{\mathbf{z}}}{c} \right\} \quad (3)$$

is the radiation reaction term. We will follow the ideas described in Sec. 10 in Ref. [47] (see Sec. 10.3 in particular) for treating the radiation reaction term, and considering it a perturbation term to the full equation of motion. Moreover, for most of the simulations reported here, where generally  $|\dot{\mathbf{z}}|/c \ll 1$ , we will follow the conventional nonrelativistic approximation of  $\mathbf{R}_{\text{reac}} \approx \frac{2}{3} \frac{e^2}{c^3} \frac{d^3 \mathbf{z}}{dt^3}$ . Using a perturbative treatment, then

$$\mathbf{R}_{\text{reac}} \approx \frac{2}{3} \frac{e^2}{c^3} \frac{d^3 \mathbf{z}}{dt^3} \approx \frac{2}{3} \frac{e^2}{c^3} \frac{d}{dt} \left[ \frac{1}{m} \left( -\frac{e^2 \mathbf{z}}{|\mathbf{z}|^3} - e \left\{ \mathbf{E}[\mathbf{z}(t), t] + \frac{\dot{\mathbf{z}}}{c} \times \mathbf{B}[\mathbf{z}(t), t] \right\} \right) \right] \quad . \quad (4)$$

A number of numerical approaches were examined, including a “leapfrog scheme,” as described in Chap. 4 in Ref. [49], an adaptive stepsize fifth-order Runge-Kutta routine [50], and the Bulirsch-Stoer (BS) method with an adaptive step control [50]. The last approach has been found to be particularly robust compared with the other routines, with typically substantially smaller CPU times, and much larger step sizes for the same numerical accuracy conditions, under a wide variety of different applied electromagnetic radiation situations.

The numerical solution of Eq. (2) was implemented by treating it as six first order differential equations, with  $\mathbf{p} = m\gamma\dot{\mathbf{z}}$  inverted to

$$\dot{\mathbf{z}} = \frac{\mathbf{p}}{m \left[ 1 + \left( \frac{\mathbf{p}}{mc} \right)^2 \right]^{1/2}} , \quad (5)$$

and

$$\dot{\mathbf{p}} = -\frac{e^2\mathbf{z}}{|\mathbf{z}|^3} + \mathbf{R}_{\text{reac}} + (-e) \left\{ \mathbf{E}[\mathbf{z}(t), t] + \frac{\dot{\mathbf{z}}}{c} \times \mathbf{B}[\mathbf{z}(t), t] \right\} , \quad (6)$$

where the right sides of the above two equations were expressed in terms of  $\mathbf{z}(t)$  and  $\mathbf{p}(t)$ , including  $\mathbf{R}_{\text{reac}}$  in Eq. (4). Using Cartesian coordinates, with  $u_1 = z_1 = x$ ,  $u_2 = z_2 = y$ ,  $u_3 = z_3 = z$ ,  $u_4 = p_1 = p_x$ ,  $u_5 = p_2 = p_y$ ,  $u_6 = p_3 = p_z$ , then  $\dot{u}_i$  for  $i = 1, 2, 3$  is given by Eq. (5) and  $\dot{u}_i$  for  $i = 4, 5, 6$  is given by Eq. (6).

For most results that will be reported in the present article, which largely involve conditions with  $|\dot{\mathbf{z}}|/c \ll 1$ , the nonrelativistic approximation of  $\mathbf{p} = m\gamma\dot{\mathbf{z}} \approx m\dot{\mathbf{z}}$  in the simulations make fairly little difference. Of course the appropriate use of relativistic dynamics is important if sufficiently high speeds are examined; however, we also found that if orbits are observed for sufficiently long times periods, the character of the trajectories can change quite differently when the dynamics is treated relativistically versus nonrelativistically. Our plan is to emphasize these differences in a later publication. For the present article, nearly all results shown in figures would be altered only very slightly if relativistic rather than non-relativistic dynamics were used, largely because speeds considered here were generally not so large, nor times so long, that these effects became important. Hence, for the present article, we will stick with nonrelativistic analysis, and will plan to analyze situations in later publications where this distinction becomes important to make. Hence, here we can treat Eq. (5) as  $\dot{\mathbf{z}} = \mathbf{p}/m$ .



### III. INITIAL NUMERICAL STUDY ON STABILITY

We begin by showing numerical results for the collapse of a classical electron's orbit. This result was viewed by physicists around 1900 as being a serious problem for classical physics being able to properly account for the stability of a atom consisting of electrons orbiting more massive and oppositely charged nuclei. Maxwell's equations require that as charges accelerate or decelerate, electromagnetic energy must be radiated; an orbiting electron must then spiral into the nucleus in order for the total sum of kinetic energy, the potential energy between the nucleus and the electron, and the radiated electromagnetic energy, to be conserved. The LD equation predicts this result nicely.

Figure 1 shows what the LD equation predicts for a classical electron initially in a circular orbit of radius  $r \equiv |\mathbf{z}| = 0.5 \text{ \AA}$  about an infinitely massive nuclei of charge  $+e$ . As can be seen, the time of collapse of the electron in this classical hydrogen model is somewhat larger than  $1.3 \times 10^{-11}$  sec. Since the Bohr radius of  $a_B \equiv \hbar^2 / (me^2) = 0.52917 \text{ \AA}$  is the average radius of hydrogen in its ground state, as predicted by quantum mechanics (QM), then this numerical result clearly shows the huge discrepancy of this simple classical model versus the obvious physical result of stable hydrogen atoms in nature.

Of course, if we were to treat the nucleus as a finite mass, with a mass of about 1836 times that of the orbiting electron, then we would have a somewhat more accurate model of hydrogen, and we would then want to treat the problem using a center of mass coordinate system. However, for the purposes of this article, and for the results that will be displayed, such considerations are really quite secondary, so, we will not enter into them here.

We now turn to examining what might happen to this simple atomic system when radiation acts on the system. One of us (Cole) has, some time ago, done lengthy numerical experiments attempting to simulate the effects of classical electromagnetic ZP radiation. The difficulties arise from a number of perspectives, including the need to simulate for long periods of time (millions of orbits) without incurring undue numerical errors, while at the same time attempting to adequately capture the physical effects of this singular radiation field, whose spectrum increases monotonically in magnitude with frequency.

However, despite these complications, we have made progress on a much simpler front involving what happens to a classical electron in a near circular orbit when in interaction with a single, or a set, of circularly polarized (CP) electromagnetic plane waves. Despite

the simplicity of this consideration, the nonlinear results are in many ways quite surprising. Moreover, we think the following considerations may reveal at least a partial insight into some of the more important aspects of the dynamics of a classical hydrogen atom acted upon by a more complicated radiation field, and should also shed insight into controlling the excitation, ionization, and stabilization of electrons in Rydberg atomic states.

To begin, we consider the simple idea of designing an incident radiation state on the orbiting electron in a circular orbit to balance the effect of radiation reaction, so that the only net force acting on the orbiting electron is the Coulombic attractive force of the nucleus. Here we will not try to make a perfect balance, as we do not expect to be able to balance the  $(-e)\dot{\mathbf{z}} \times \mathbf{B}/c$  part of the Lorentz force, nor the second order effects that occur in the radiation reaction term. However, we can achieve a near balance in the following way. In a circular orbit, with radial and tangential unit vectors  $\hat{\mathbf{r}}$  and  $\hat{\theta}$ , then  $\mathbf{z}(t) = r\hat{\mathbf{r}}(t)$ , with  $r$  a constant, and then  $\frac{d}{dt}\hat{\mathbf{r}} = \frac{d\theta}{dt}\hat{\theta}$ , and  $\frac{d}{dt}\hat{\theta} = -\hat{\mathbf{r}}\frac{d\theta}{dt}$ . From Eq. (4), and approximating  $\frac{d^3\mathbf{z}}{dt^3}$  as in the nonrelativistic case as  $\frac{d}{dt}\left(-\frac{e^2\mathbf{z}}{m|\mathbf{z}|^3}\right)$ , since the dominate force on the orbiting electron is in this case the Coulombic attractive force, then

$$\frac{d}{dt}\left(-\frac{1}{m}\frac{e^2\mathbf{z}}{|\mathbf{z}|^3}\right) = -\frac{e^2}{m}\left[\frac{\frac{d\mathbf{z}}{dt}}{|\mathbf{z}|^3} - \frac{3\mathbf{z}(\mathbf{z}\cdot\frac{d\mathbf{z}}{dt})}{|\mathbf{z}|^5}\right]. \quad (7)$$

For circular motion,  $\mathbf{z}\cdot\frac{d\mathbf{z}}{dt} = 0$ , so:

$$\mathbf{R}_{\text{reac}} \approx -\frac{2}{3}\frac{e^4\omega}{mc^3r^2}\hat{\theta}, \quad (8)$$

where  $\omega \equiv d\theta/dt$  is a constant. Thus, for circular motion the radiation reaction force acts in the direction opposite to the velocity of the electron, like a simple drag force. By designing a radiation state acting on the orbiting electron to counteract the radiation reaction, then circular motion will be maintained by satisfying conventional Newtonian mechanics. Specifically, by equating the Coulombic attraction of  $-e^2\hat{\mathbf{r}}/|\mathbf{z}|^2$  to  $m\ddot{\mathbf{z}} = -mr\omega^2\hat{\mathbf{r}}$  in the nonrelativistic case, one obtains that

$$\omega = \left(\frac{e^2}{mr^3}\right)^{1/2}. \quad (9)$$

For relativistic motion, where  $\frac{d}{dt}(\gamma m\dot{\mathbf{z}}) = -e^2\mathbf{z}/|\mathbf{z}|^3$ , then to maintain circular motion, the angular frequency needs to be given by

$$\omega = \left(\frac{e^2}{mr^3}\right)^{1/2} \left\{ \left[ 1 + \left(\frac{e^2}{2c^2mr}\right)^2 \right]^{1/2} - \frac{e^2}{2c^2mr} \right\}^{1/2}. \quad (10)$$

A very simple way of satisfying this condition of balancing the radiation reaction for a circular orbit is to have a CP plane wave propagate in the direction perpendicular to the plane of the electron orbit, with an angular frequency given by Eq. (10), or approximately by Eq. (9) in the nonrelativistic case, such that  $-e$  times the electric field is opposite to  $\mathbf{R}_{\text{reac}}$  in Eq. (8), or

$$A = \frac{2}{3} \frac{e^3 \omega}{mc^3 r^2} , \quad (11)$$

where  $A$  is the amplitude of this circular polarized plane wave.

Such a CP electromagnetic plane wave will negate the major component of the radiation reaction and will then provide a stable circular orbit, until second order effects accumulate sufficiently that the plane wave and orbiting electron fall far enough out of phase with respect to each other. Using our simple method, we cannot expect a perfectly balanced orbit, even when the relativistic frequency effect in Eq. (10) is taken into account, because of three reasons: (1) We balanced the radiation reaction by considering the Lorentz force contribution of  $-e\mathbf{E}[\mathbf{z}(t), t]$ , where  $\mathbf{E}[\mathbf{z}(t), t]$  is the electric field of the CP plane wave. We did not take into account the other Lorentz force component of the plane wave, namely,  $-e\frac{\dot{\mathbf{z}}}{c} \times \mathbf{B}[\mathbf{z}(t), t]$ . For nonrelativistic motion, this effect is small, however. Moreover, since  $\mathbf{B}$  will be directed along the radial direction, and  $\dot{\mathbf{z}}$  is along  $\hat{\theta}$ , then this Lorentz force component is normal to the plane of the orbit, thereby acting to accelerate the electron in this direction and in this way acting to eventually put the electron out of phase with respect to the incident plane wave. (2) We only attempted to balance the radiation reaction contribution of  $-e^2\mathbf{z}/|\mathbf{z}|^3$  in Eq. (4), rather than also the second order effect of the plane wave  $-e\{\mathbf{E}[\mathbf{z}(t), t] + \frac{\dot{\mathbf{z}}}{c} \times \mathbf{B}[\mathbf{z}(t), t]\}$  in Eq. (4). This should be, under most situations, a very small effect. (3) We used the nonrelativistic approximation for the radiation reaction force of  $\mathbf{R}_{\text{reac}} \approx \frac{2}{3} \frac{e^2}{c^3} \ddot{\mathbf{z}}$  in Eq. (3), rather than taking into account other relativistic effects in this term. For the speeds considered in the present study, this approximation should be quite good.

Figure 2 contains plots of radius ( $r$ ) versus time ( $t$ ) for situations of CP plane waves with different amplitudes, where the electron starts in a circular orbit of radius  $0.5 \text{ \AA}$ . In these plots, the Lorentz force component of the plane wave, namely,  $-e\frac{\dot{\mathbf{z}}}{c} \times \mathbf{B}[\mathbf{z}(t), t]$ , is taken into account in deducing the trajectory of the orbiting electron. Moreover, the Lorentz force part due to the applied CP wave acting on the orbiting electron, namely,  $-e\{\mathbf{E}[\mathbf{z}(t), t] + \frac{\dot{\mathbf{z}}}{c} \times \mathbf{B}[\mathbf{z}(t), t]\}$  in Eq. (4), was taken into account in the radiation reaction.

The bottom curve in Fig. 2 is just a subsection of the curve in Fig. 1. As can be seen, when the amplitude of the CP plane wave meets the condition of Eq. (11), then stability is achieved. Figure 2 also shows how the stability condition is approached as the amplitude of the applied electric field is increased. It should be noted that the period of the orbiting electron is approximately  $T = \frac{2\pi}{\omega} \approx 2\pi \left( \frac{e^2}{mr^3} \right)^{1/2} \approx 1.4 \times 10^{-16}$  sec, so approximately 3600 orbits are contained in Fig. 2.

#### IV. NUMERICAL STUDY INVOLVING MORE COMPLEX STABILITY CONDITIONS

The previous section simply confirmed the idea that an incident radiation state could be chosen to provide reasonable stability to the orbit of a classical charged particle in a Coulombic binding potential. Without doubt, the situation chosen was highly idealized. Changes to the direction of propagation of the incident radiation, to the plane of the orbit, and/or changes in the phase or of the frequency of the incident radiation would have devastating effects for achieving the stability shown in Fig. 2. Moreover, only an idealized circular orbit was examined here. In later work, we will examine the more general situation of elliptic orbits. As will be shown there, much more complicated radiation states are required, but stability effects can still be observed.

What we now want to turn to is an examination of what happens if the amplitude of the electric field of the CP plane wave is increased *above* the value of Eq. (11). This situation now becomes significantly more difficult to predict what will happen; indeed, now a numerical study seems essential to fully analyze this problem. Figure 3 shows our results. When the amplitude of the electric field exceeds the critical value in Eq. (11), a stability condition still exists, although in a much different form, as oscillations in the  $r$  versus  $t$  curve become very prominent. As the amplitude of the electric field increases, the amplitude of the radial “oscillations” increase, as does their frequency. It should be noted, though, that in each period of radial “oscillation,” there are still many revolutions of the charged particle about the nucleus, at least for the cases examined here. When  $A = 10$  statvolts, then about 960 revolutions occur per radial oscillation period. When  $A = 100$ , there are about 570 such revolutions, or about a 60% decrease in radial oscillation period from the  $A = 10$  statvolt case, while the amplitude of the radial oscillations increases by a factor of about

5.5 from the  $A = 10$  statvolt situation. Clearly some very nonlinear results are occurring. Figure 4 summarizes this aspect of this nonlinear reaction to the electric field amplitude  $A$  of the CP incident plane wave.

What is most significant, however, is that stability does exist when  $A > \frac{2}{3} \frac{e^3 \omega}{mc^3 r^2}$ . This interesting observation opens up a number of possibilities, both for a slightly deeper insight into the possible theoretical underpinnings of SED, as well as for practical applications of manipulating Rydberg atomic systems with applied radiation fields, in situations where a classical or semiclassical analysis will likely hold. Hence, a deeper understanding of what is going on in Fig. 3 seems essential. We now proceed with that analysis.

When the electric vector of the CP plane wave is oriented along the opposite direction of the  $-e$  charged orbiting electron, then positive work is done by the CP plane wave on the  $-e$  charge. The sum of the kinetic plus potential energy of the orbiting particle must then increase, resulting in  $r$  becoming larger by having the particle slowly spiral outward. The particle still follows a nearly circular orbit, but the radius of the circle slowly increases. As this happens, the period of the orbit increases. This change in period of the orbiting particle, as opposed to the fixed frequency of the applied CP plane wave, causes the  $\mathbf{E}$  vector and the velocity  $\dot{\mathbf{z}}$  to become out of phase, so that they eventually begin to oppose one another. At this point the CP plane wave begins to do negative work on the orbiting particle and  $r$  begins to slowly decrease by having the particle being to spiral inward toward the nucleus. As  $r$  decreases, the period of each revolution of the electron around the nucleus decreases; eventually the  $\mathbf{E}$  field and the velocity come back into phase. When this happens, positive work can again be done on the orbiting particle to again increase  $r$ . This pattern of increasing and decreasing spirals can continue for a significantly long time, well beyond the time of  $5 \times 10^{-13}$  sec in Fig. 3, before the  $\mathbf{E}$  field and the velocity are no longer able to come back into phase. (This effect will be illustrated in the next section.) At this point,  $r$  will simply continue to decrease, and stability is no longer possible.

This simple explanation can also be used to qualitatively understand a number of other features. For example, the period of the oscillations of  $r$  versus  $t$  becomes smaller as  $A$  is increased (see Fig. 4), since the maximum rate of work by the CP plane wave increases as  $A$  increases, so the average radius will increase and decrease faster when  $A$  is larger. Also, the larger the amplitude  $A$  is, the larger will be the amplitude of the oscillations in radius versus time, as more work can be done on the spiraling electron before it revolves enough

times to become out of phase with the CP wave. Figure 4 shows these effects.

Figure 5 provides more quantitative information, using the  $A = 100$  statvolt situation as a vehicle for explanation. Two curves are shown, superimposed on top of each other; they both have the same time scale on the  $x$ -axis, namely, the beginning of the  $A = 100$  statvolt curve in Fig. 3. One curve shows  $r$  versus  $t$ , just as in Fig. 3. The other displays the following quantity as a function of time, namely,

$$F_v \equiv (-e) \left\{ \mathbf{E} [\mathbf{z}(t), t] + \frac{\dot{\mathbf{z}}}{c} \times \mathbf{B} [\mathbf{z}(t), t] \right\} \cdot \frac{\dot{\mathbf{z}}}{|\dot{\mathbf{z}}|} ,$$

which is the component of the force of the CP plane wave acting along the particle's velocity direction, or, it is also the rate of work done by the CP plane wave on the orbiting particle, normalized by the velocity.

As can be seen from Fig. 5, when  $F_v$  is positive,  $r$  increases, since positive work is being done on the particle. As the radius increases initially,  $F_v$  becomes smaller, since  $e\mathbf{E}$  becomes mismatched with  $\dot{\mathbf{z}}$ . During this period,  $r$  continues to increase, although its rate of increase slows as  $F_v$  becomes smaller. At slightly past  $1 \times 10^{-14}$  sec,  $F_v$  changes sign, becoming negative, causing  $r$  to begin decreasing. This decrease now starts making the orbital period decrease, eventually bringing the electric field and velocity back into phase.  $F_v$  then becomes positive (around  $3 \times 10^{-14}$  sec), at which point  $r$  again begins to increase.

It is interesting to note, however, that the average of  $F_v$  is not zero; instead, it is positive, as can be seen by comparing the areas of the two regions with hatched marks in Fig. 5 (the left region is wider). Consequently, the average of  $(-e) \mathbf{E} \cdot \dot{\mathbf{z}} = F_v |\dot{\mathbf{z}}|$ , is positive, since  $|\dot{\mathbf{z}}|$  is nearly constant. Hence, despite successive periods of positive rates of work, followed sequentially by negative rates of work, the net average work done by the applied field on the particle per every cycle in Fig. 5 (about  $4 \times 10^{-14}$  sec), is positive. This result is as it should be, since in order for this classical orbiting electron to maintain, on average, a "stable" orbit, then it must continually radiate energy. Via the laws of classical electrodynamics, an accelerating charge must radiate electromagnetic energy, which is what we see happening here. Indeed, if one calculates the average radiated energy by the orbiting electron, per cycle, it precisely equals the average positive work done by the applied field on the particle. Hence, of course, energy is indeed conserved; the radiated energy is precisely compensated by the work of the applied field.

Figure 6(a) shows the  $A = 100$  statvolts case of  $r$  versus  $t$  taken out much farther in

time, to  $5 \times 10^{-12}$  sec, which includes about 36000 orbits. The orbit remains remarkably stable, particularly in comparison to the dramatic difference with the  $A = 0$  statvolts curve also shown in Fig. 6(a). However, as can be seen in Fig. 6(b), which zooms in on Fig. 6(a) around  $r = 0.5 \text{ \AA}$  on the  $y$ -axis, the envelope of this curve slowly increases in width. This seems to be a common feature of the  $r$  versus  $t$  curves for different values of  $A$ , as well as in numerical experiments we have carried out for a large number of other situations, where in some cases a huge family of applied CP plane waves act on the orbiting particle, with some at near resonance with the orbiting particle. The orbiting particle gradually spirals inward to smaller radii values, and outer to larger radii values, until the orbiting electron versus the fixed frequency CP plane wave are not able to come back into phase with each other again.

In the case of a single CP plane wave, the particle's orbit will eventually decay. If the orbiting particle and the  $\mathbf{E}$  field of the CP wave are initially in phase, however, the length of time before decay occurs can be extremely long. For example, for the  $A = 100$  statvolt case, our simulations reveal a time of nearly  $1.5 \times 10^{-11}$  sec before decay begins, which is a longer time than the total decay shown in Fig. 1. When one varies the conditions  $A$ , the initial phase, and a family of CP wave, then a wide variety of interesting results can be obtained. We intend to present more of these results in future work. For now, though, perhaps the key point to be made is that by varying the initial phase of the  $\mathbf{E}$  field of the CP wave, we can move the point at which decay begins closer in to the origin, to enable easier examination of the interesting behavior that occurs when decay does begin. Indeed, the subsequent example and discussion appears to apply fairly generically to a range of conditions where an initial stable-like condition is created, but which eventually changes in character to a decaying behavior.

In Fig. 6,  $(-e)\mathbf{E}$  and  $\dot{\mathbf{z}}$  were pointing in the same direction at time  $t = 0$ . If one chooses them to be perpendicular to each other initially, or  $\pi/2$  out of phase with respect to each other, so that the electric field cannot help to counteract the dissipative force  $\mathbf{R}_{\text{reac}}$ , then the orbit will decay almost immediately. For phases chosen between these two extremes of  $\phi = 0$  (Fig. 6) and  $\phi = \pi/2$ , stability will be maintained, but for progressively shorter times for increasing values of  $\phi$ , thereby mimicking the eventual decaying behavior that occurs for  $\phi = 0$ , but at much smaller values of time.

For example, in Fig. 7, the initial phase difference was chosen to be  $\pi/4$ . In this plot, we see the trajectory of the orbiting particle starts out in the usual cycle of radially spiraling

in and out, but then at a time of about  $3.2 \times 10^{-12}$  sec, the orbit in Fig. 7(a) suddenly changes to one of decay, where it then closely parallels the other curve shown in Fig. 7(a), where only the radiation reaction force acts. Figure 7(b) blows up the region around  $r = 0.5$  Å. As can be seen, the same pattern we saw in Fig. 6(b) occurs, where the envelope of the  $r$  versus  $t$  curve grows in width. Indeed, Fig. 7(b) is very similar to Fig. 6(b), but simply farther out to the right in time than what is shown in Fig. 6(b). In Fig. 7(b), as in Fig. 6(b), the envelope curve again increases in size, starting at a wider width than in Fig. 6(b), and continuing until the trajectory reaches a point where stability can no longer be enforced; an abrupt change in the orbit then occurs. Figure 7(c) zooms into the region where this transition point occurs. If one was to watch an  $x - y$  “movie” of the orbiting particle, corresponding to Fig. 7, as a function of time, one would see the particle spiral out, then in, then out, etc., about a nearly circular orbit of radius 0.5 Å, until finally the particle only spirals out up to the  $r = 0.5$  Å point at  $t = 3.227$  sec. After that point of  $t \gtrsim 3.227$  sec [see Fig. 7(c)], the electron continues to spirals in and out, but on average it only spirals inward.

Figure 8 analyzes this behavior in more detail. In Fig. 8(a), the corresponding time regime to Fig. 7(c) is shown, but now  $F_v$  vs.  $t$  is shown. To the left of the transition-decay point at  $t = 3.2 \times 10^{-12}$  sec, each positive region of  $F_v$  has two humps and one minima, while each negative region of  $F_v$  looks like an inverted, but smaller, corresponding section of the positive region. To the right of the decay point, this  $F_v$  vs.  $t$  changes dramatically, as the positive and negative regions of  $F_v$  all have single sequential maxima and minima.

Figure 8(b) zooms in on the transition point in Fig. 8(a). Two curves are superimposed here, namely,  $r$  vs.  $t$ , and  $F_v$  vs.  $t$ . Also, vertical lines are drawn that separate the  $F_v < 0$  regions from the  $F_v > 0$  regions. As can be seen, whenever  $F_v < 0$ , then the radius decreases, as the orbiting classical electron spirals inward; when  $F_v > 0$ , just the opposite happens. To the left of the transition point at  $t = 3.2 \times 10^{-12}$  sec, the average work by work done by the CP wave in the spiraling-out regions, versus the average work done by the CP wave in the spiraling-in regions, are enough to compensate for the radiation that is continually given off by the orbiting classical electron (qualitatively, the width of the  $F_v > 0$  region is much wider than the  $F_v < 0$  region to the left of  $3.26 \times 10^{-12}$  sec, while the heights are nearly equal). More specifically, to the left of the transition point, there are sequential regions where the CP wave does not provide enough work to prevent radial-spiraling inward (the



$F_v < 0$  regions), followed by regions (the  $F_v > 0$  regions) where the CP wave provides too much work on the electron, so a radial spiraling outward behavior follows; the net result is an average net amount of positive work per cycle, just enough to compensate for the energy that is continually being radiated by the orbiting electron. However, to the right of about  $t = 3.26 \times 10^{-12}$  sec, this is not the case, as one can see qualitatively from Fig. 8(b), as the positive areas of the  $F_v$  curve to the right of the transition point are nearly equal in area to the negative regions. Hence, in this region, the phase of the orbiting classical electron versus the applied electric field have become sufficiently out of phase, that  $\mathbf{E}$  cannot do adequate work on the orbiting charge to prevent its radial collapse due to its energy loss from electromagnetic radiated energy.

To further illustrate, Fig. 8(c) shows a superposition of  $r$  vs.  $t$  and  $F_v$  vs.  $t$ , for the same trajectory of this  $A = 100$  statvolt,  $\phi = \pi/4$  case, but as occurs near  $t = 0$ . As can be seen, early on, well away from when the inward spiraling-transition occurs, very regular, periodic regions of double humped periods occur, which are well explained by the sign of the corresponding  $F_v$  regions. At the transition point in Fig. 8(b), the change in shape is very dramatic.

## V. SUGGESTIVE SITUATIONS

Many other numerical experiments can be carried out to examine the detailed nonlinear behavior of this physically very simple, yet dynamically very complicated, classical electrodynamic system. Here we show two more situations. First, in Fig. 9(a), we have superimposed four  $r$  vs.  $t$  curves, one with  $A = 0$ , and three involving a single CP plane wave of  $A = 100$  statvolts acting on the orbiting particle. The latter three curves have different initial phases between the orbiting electron and the electric field. As can be seen, when the initial phase difference is  $\frac{1}{2}\pi$ , the electron immediately begins a spiraling, decaying orbit, that is centered just to the left of the curve that would be followed in the  $A = 0$  situation [see Fig. 9(b)]. Hence in this situation, from the very beginning, the electric field is not able to significantly aid the classical electron, although, as shown in Fig. 9(b), there still exist subsequent regions where positive and negative work is done by the CP wave to both aid and hinder the decaying orbit, resulting in an orbit oscillating about a trajectory that parallels the purely decaying one of  $A = 0$ .

In the other two curves in Fig. 9(a), where  $\phi = \frac{3}{8}\pi$  and  $\phi = \frac{1}{4}\pi$ , a very similar scenario results, but, the trajectory simply looks like it has been displaced to the right. Indeed, what is particularly interesting is what is shown in Fig. 9(c), where the  $\phi = \frac{3}{8}\pi$  curve is superimposed right over the  $\phi = \frac{1}{2}\pi$  curve, such that the transition points line up. What is particularly interesting here is the nearly identical behavior at this transition point, despite a huge difference in time displacement. In rough terms, clearly the transitory difference in behavior between the curves has died out, and only the forced motion due to the applied CP wave is what dictates the observed, nearly identical behavior.

Figure 10(a) shows yet another interesting observation, where the electron is started in a circular orbit from three different radii, and allowed to decay in its orbit. In each case, the same identical CP plane wave, with  $A = 100$  statvolt,  $\phi = 0$ , is acting on the orbiting classical electron, from the very beginning of its trajectory. The frequency of this wave corresponds to the orbital frequency of the electron at the radius of  $0.5 \text{ \AA}$ . Also superimposed, is the corresponding  $A = 0$  curve. As can be seen, in each of the three  $A = 100$  statvolt curves, the CP wave has progressively more and more influence on the decaying orbit, as the electron approaches the  $r = 0.5 \text{ \AA}$  point. Of course, this is precisely what one would expect from the study of forced, damped, simple harmonic motion: when the forcing term (in this case, the CP wave) is at the same frequency as the “natural harmonic frequency” of a resonator, the response will be the largest.

However, what is interesting here, is the degree of response, and the degree that the response tapers off as the two become out of resonance with each other. Without detailed simulation, it seems that such insight and knowledge about this highly nonlinear system would be difficult to predict. Figure 10(b) zooms in on the middle trajectory near the transition point, where a resonant-like behavior is seen to occur. This plot gives one some idea of the “bandwidth” of the effect of a CP plane wave with one frequency, that acts upon a particle orbiting at another frequency. Possibly by judiciously choosing the phase and amplitude of  $\mathbf{E}$  at  $t = 0$ , one could actually “catch” the classical electron at  $0.5 \text{ \AA}$  and “hold” it before it’s orbit again falls into the characteristic decay pattern shown.

Thus, even with this simple nonlinear system, involving only one CP plane wave, the variables of initial phase, amplitude, and starting radii, all have key effects. This study doesn’t even touch on the far more complicated behavior of superimposing the effects of other CP waves, of different amplitudes and phases, nor of examining the dynamic responses of

the orbiting electron corresponding to noncircular initial orbits. To date, we have made a number of such investigations and have found very interesting and suggestive results. We hope to report on these results in the future.

## VI. CONCLUDING REMARKS

Our simulation study here of a classical electron starting in near-circular orbits around a classical  $+e$  charged, infinitely massive nucleus, reveals a number of interesting nonlinear dynamical effects. In all cases, we have examined orbits following the Lorentz-Dirac equation, treating the orbiting particle with the usual numerical approximation for radiation reaction (see Sec. 10.3 in Ref. [47]). We believe our results will be helpful for future developments involving studies and applications entailing the use of Rydberg-like atomic systems, as well as of interest for more theoretical studies, such as in the area of SED.

Much of the work we presented in the present article is important for understanding the basics of much more complicated situations involving the same classical hydrogen system, but where families of CP plane waves are applied, with distributions of varying amplitude, phase, and propagation direction, and where the initial orbit of the classical electron is noncircular. Indeed, we have examined situations of families of thousands of CP waves simultaneously acting on the orbiting electron. One feature of such studies, in common with the work reported in this article, is that, without question, near stability-like conditions can be achieved for classical electrons in orbits about a classical nucleus, by having electromagnetic radiation act on the orbiting charge to counterbalance the effects of radiation reaction. This result should not come as a surprise, since the idea is very clear, and probably has been recognized by many physicists, many times over throughout the years. Section III went over this basic idea. However, what will undoubtedly come as a surprise to most physicists, is that there exists a huge range of additional near-stability conditions, aside from this very precise point described by Eq. (11). Even when considering just a single CP wave, we have seen in the present study where the amplitude of the CP wave may be much larger than the value in Eq. (11), and where the initial phase can be varied considerably, yet dynamic stabilities can still result [see Figs. 3, 6, and 9(a)]. Such situations can also occur when large families of CP plane waves are applied.

A second common feature of the work presented here, and the work we intend to report

on in the future, is that CP plane waves certainly have their greatest influence on an orbiting electron when the frequency of the wave, and the frequencies describing the orbit (as in an elliptical orbit), most closely correspond. Again, this should not come as a surprise, but, the precise magnitude of the effect, under various conditions, is certainly nontrivial to determine. Further study here should be helpful for applications in scientific and technological advances [1]-[15], under situations where classical and semiclassical dynamics may be applied, as well as for deeper insight into the fully classical theory of SED [43],[44].

Third, when an orbiting electron is in some form of stable resonance, then the radial range of the orbiting electron tends to broaden out with time, as seen for example in Figs. 6(b) and 7(b). We find this same behavior to occur in much more complicated scenarios with large families of applied CP waves. Moreover, additional interesting situations can be achieved in such cases, including the “catching” of a decaying electron, in a similar, but much more dramatic behavior than shown in Fig. 10(a), as well as making an electron’s average radial orbit increase in a jump-like step.

Thus, we believe our present study to be the beginning of interesting investigations, guided by simulation, on this very nonlinear, yet simple, classical electrodynamic system.

- 
- [1] W. Clark and C. H. Greene. Adventures of a rydberg electron in an anisotropic world. *Rev. Mod. Physics*, 71(3):821–833, 1999.
- [2] P. A. Braun. Discrete semiclassical methods in the theory of rydberg atoms in external fields. *Rev. Mod. Phys.*, 65(1):115–161, 1993.
- [3] J. A. Griffiths and D. Farrelly. Ionization of rydberg atoms by circularly and elliptically polarized microwave fields. *Phys. Rev. A*, 45(5):R2678–R2681, 1992.
- [4] J. Grochmalicki, M. Lewenstein, and K. Rzazewski. Stabilization of atoms in superintense laser fields: Is it real? *Phys. Rev. Lett.*, 66(8):1038–1041, 1991.
- [5] C. Wesdorp, F. Robicheaux, and L. D. Noordam. Displacing rydberg electrons: The mono-cycle nature of half-cycle pulses. *Phys. Rev. Lett.*, 87(8):083001, 2001.
- [6] S. Yoshida, C. O. Reinhold, P. Kristofel, and J. Burgdorfer. Exponential and nonexponential localization of the one-dimensional periodically kicked rydberg atom. *Phys. Rev. A*, 62:023408, 2000.
- [7] G. N. Rockwell, V. F. Hoffman, Th. Clausen, and R. Blumel. Realistic three-dimensional computations of microwave-ionization curves of hydrogen rydberg atoms. *Phys. Rev. A*, 65:025401, 2002.
- [8] P. M. Koch and K. A. H. van Leeuwen. The importance of resonances in microwave “ionization” of excited hydrogen atoms. *Physics Reports*, 255:289–403, 1995.
- [9] J. G. Leopold and I. C. Percival. Microwave ionization and excitation of rydberg atoms. *Phys. Rev. Lett.*, 41(14):944–947, 1978.
- [10] M. W. Noel, W. M. Griffith, and T. F. Gallagher. Classical subharmonic resonances in microwave ionization of lithium rydberg atoms. *Phys. Rev. A*, 62:063401, 2000.
- [11] T. F. Gallagher, R. M. Hill, and S. A. Edelstein. Method and apparatus for field ionization for isotope separation. *US Patent No. 4,070,580*; see: [www.uspto.gov](http://www.uspto.gov), pages 1–7, 1978.
- [12] R. Bir and J. P. Schermann. Method of isotope separation. *US Patent No. 4,360,501*; see: [www.uspto.gov](http://www.uspto.gov), pages 1–6, 1982.
- [13] T. Oomori, K. Ono, and S. Fujita. Ion current generator system for thin film formation, ion implantation, etching and sputtering. *US Patent No. 4,893,019*; see: [www.uspto.gov](http://www.uspto.gov), pages 1–43, 1990.

- [14] T. Oomori and K. Ono. Ion source. *US Patent No. 5,115,135*; see: [www.uspto.gov](http://www.uspto.gov), pages 1–75, 1992.
- [15] L. D. Noordam and M. D. Lankhuijzen. Apparatus for detecting a photon pulse. *US Patent No. 6,049,079*; see: [www.uspto.gov](http://www.uspto.gov), pages 1–9, 2000.
- [16] D. C. Cole. Reviewing and extending some recent work on stochastic electrodynamics. pages 501–532. World Scientific, Singapore, 1993.
- [17] L. de la Peña and A. M. Cetto. *The Quantum Dice - An Introduction to Stochastic Electrodynamics*. Kluwer Acad. Publishers, Kluwer Dordrecht, 1996.
- [18] T. H. Boyer. Random electrodynamics: The theory of classical electrodynamics with classical electromagnetic zero-point radiation. *Phys. Rev. D*, 11(4):790–808, 1975.
- [19] T. H. Boyer. The classical vacuum. *Sci. American*, 253:70, August 1985.
- [20] D. C. Cole. Derivation of the classical electromagnetic zero-point radiation spectrum via a classical thermodynamic operation involving van der waals forces. *Phys. Rev. A*, 42:1847–1862, 1990.
- [21] T. W. Marshall. Random electrodynamicis. *Proc. R. Soc. London, Ser. A*, 276:475–491, 1963.
- [22] T. W. Marshall. Statistical electrodynamics. *Proc. Camb. Phil. Soc.*, 61:537–546, 1965.
- [23] T. H. Boyer. Derivation of the blackbody radiation spectrum without quantum assumptions. *Phys. Rev.*, 182:1374–1383, 1969.
- [24] T. H. Boyer. Classical statistical thermodynamics and electromagnetic zero-point radiation. *Phys. Rev.*, 186:1304–1318, 1969.
- [25] D. C. Cole and A. Rueda. The quantum dice: An introduction to stochastic electrodynamics. *Found. Phys.*, 26:1559–1562, 1996.
- [26] D. C. Cole. Reinvestigation of the thermodynamics of blackbody radiation via classical physics. *Phys. Rev. A*, 45:8471–8489, 1992.
- [27] D. C. Cole. Thermodynamics of blackbody radiation via classical physics for arbitrarily shaped cavities with perfectly conducting walls. *Found. Phys.*, 30(11):1849–1867, 2000.
- [28] H. M. Franca and T. W. Marshall. Excited states in stochastic electrodynamics. *Phys. Rev. A*, 38(7):3258–3263, 1988.
- [29] T. H. Boyer. Thermal effects of acceleration through random classical radiation. *Phys. Rev. D*, 21(8):2137–2148, 1980.
- [30] T. H. Boyer. Thermal effects of acceleration for a classical dipole oscillator in classical elec-

- tromagnetic zero-point radiation. *Phys. Rev. D*, 29(6):1089–1095, 1984.
- [31] D. C. Cole. Properties of a classical charged harmonic oscillator accelerated through classical electromagnetic zero-point radiation. *Phys. Rev. D*, 31(8):1972–1981, 1985.
- [32] D. C. Cole. Thermal effects of acceleration for a spatially extended electromagnetic system in classical electromagnetic zero-point radiation: Transversely positioned classical oscillators. *Phys. Rev. D*, 35:562–583, 1987.
- [33] T. H. Boyer. General connection between random electrodynamics and quantum electrodynamics for free electromagnetic fields and for dipole oscillator systems. *Phys. Rev. D*, 11(4):809–830, 1975.
- [34] T. H. Boyer. Equilibrium of random classical electromagnetic radiation in the presence of a nonrelativistic nonlinear electric dipole oscillator. *Phys. Rev. D*, 13(10):2832–2845, 1976.
- [35] T. H. Boyer. Statistical equilibrium of nonrelativistic multiply periodic classical systems and random classical electromagnetic radiation. *Phys. Rev. A*, 18:1228, 1978.
- [36] R. Blanco, L. Pesquera, and E. Santos. Equilibrium between radiation and matter for classical relativistic multiperiodic systems. derivation of maxwell-boltzmann distribution from rayleigh-jeans spectrum. *Physical Review D (Particles and Fields)*, 27(6):1254–87, 15 March 1983.
- [37] R. Blanco, L. Pesquera, and E. Santos. Equilibrium between radiation and matter for classical relativistic multiperiodic systems. ii. study of radiative equilibrium with rayleigh-jeans radiation. *Physical Review D (Particles and Fields)*, 29(10):2240–54, 15 May 1984.
- [38] T.W. Marshall and P. Claverie. Stochastic electrodynamics of nonlinear systems. i. particle in a central field of force. *Journal of Mathematical Physics*, 21(7):1819–25, July 1980.
- [39] P. Claverie, L. Pesquera, and F. Soto. Existence of a constant stationary solution for the hydrogen atom problem in stochastic electrodynamics. *Physics Letters A*, 80A(2-3):113–16, 24 Nov. 1980.
- [40] A. Denis, L. Pesquera, and P. Claverie. Linear response of stochastic multiperiodic systems in stationary states with application to stochastic electrodynamics. *Physica A*, 109A(1-2):178–92, Oct.-Nov. 1981.
- [41] P. Claverie and F. Soto. Nonrecurrence of the stochastic process for the hydrogen atom problem in stochastic electrodynamics. *Journal of Mathematical Physics*, 23(5):753–9, May 1982.
- [42] D. C. Cole. Entropy and other thermodynamic properties of classical electromagnetic thermal

- radiation. *Phys. Rev. A*, 42:7006–7024, 1990.
- [43] T. H. Boyer. Scaling symmetry and thermodynamic equilibrium for classical electromagnetic radiation. *Found. Phys.*, 19:1371–1383, 1989.
- [44] D. C. Cole. Classical electrodynamic systems interacting with classical electromagnetic random radiation. *Found. Phys.*, 20:225–240, 1990.
- [45] P. A. M. Dirac. Classical theory of radiating electrons. *Proc. R. Soc. London Ser. A*, 167:148–169, 1938.
- [46] C. Teitelboim. Splitting of the maxwell tensor: Radiation reaction without advanced fields. *Phys. Rev. D*, 1(6):1572–1582, 1970.
- [47] C. Teitelboim, D. Villarroel, and Ch. G. van Weert. Classical electrodynamics of retarded fields and point particles. *Riv. del Nuovo Cimento*, 3(9):1–64, 1980.
- [48] F. Rohrlich. *Classical Charged Particles*. Addison–Wesley, MA, 1965.
- [49] R. W. Hockney and J. W. Eastwood. *Computer Simulation Using Particles*. McGraw-Hill, New York, 1988.
- [50] W. H. Press, S. A. Teukolsky, W. T. Vetterling, and B. P. Flannery. *Numerical Recipes in C: The Art of Scientific Computing*. Cambridge University Press, New York, second edition, 1992.



## Figure Captions

Figure 1: Radius vs. time ( $r$  vs.  $t$ ) for a classical model of an electron ( $m = 9.1091 \times 10^{-28}$  gm, charge  $-e$ ,  $e = 4.80298 \cdot 10^{-10}$  esu) initially in a circular orbit of radius  $0.5 \text{ \AA}$  about an infinitely massive nuclei with charge  $+e$ .

Figure 2:  $r$  vs.  $t$  for the same system as in Fig. 1, but with a CP plane wave acting on the electron, beginning in phase with the orbit of the electron, and with periodicity equal to the initial period of the orbiting electron. Each curve shows the situation for a different electric field amplitude acting, with the numerical values of  $A$  in units of statvolts. From Eq. (11), when  $A = \frac{2}{3} \frac{e^3 \omega}{mc^3 r^2} = 5.419$  statvolt, then the radius remains constant over the time period simulated.

Figure 3: (a)  $r$  vs.  $t$  for the orbiting particle, but with the amplitude of the applied CP plane wave increased beyond the critical point of Eq. (11). For  $A$  above this point ( $A = 10$  and  $100$  statvolts are shown here), the electron periodically first spirals out, then in, over and over again.  $A$  is in units of statvolts. As  $A$  increases, the radial range of the spirals increases, and the period of each spiral cycle decreases. (b)  $r$  vs.  $t$ , for  $A = 500$  statvolts. The radial range, and period of the spirals, increases significantly for this case, versus those in 3(a).

Figure 4: Two curves are shown in this plot, namely, (1) amplitude of the radial spiral (*i.e.*,  $r(t)$  minus  $r = 0.5 \text{ \AA}$ ) versus  $A$ , the amplitude of the electric field of the incident CP electromagnetic plane wave, and (2) the period of the radial spiral behavior versus  $A$ .

Figure 5: Two curves are superimposed here, both for the  $A = 100$  statvolt applied CP plane wave case. One curve shows  $r$  vs.  $t$ ; the other shows  $F_v$  versus time. When  $F_v > 0$ , it can be seen that the radius increases; when  $F_v < 0$ , the radius decreases.

Figure 6: (a)  $r$  vs.  $t$  for the  $A = 100$  statvolt CP plane wave case; also shown is the  $r$  vs.  $t$  curve when  $A = 0$ . (b) Zoomed-in view of the  $A = 100$  statvolt curve in 6(a), around the  $0.5 \text{ \AA}$  radial position. The envelope of this curve slowly increases in width.

Figure 7:  $r$  vs.  $t$  for the  $A = 100$  statvolt CP plane wave case, but with the initial phase between  $\mathbf{E}$  and  $\dot{\mathbf{z}}$  being  $\pi/4$ , rather than 0 as in Fig. 6. Also shown is the  $A = 0$  curve. (a) the  $r$  vs.  $t$  simulations are carried out to  $t = 5 \times 10^{-12}$  sec. (b) Zoomed-in view of 7(a), near the decay-transition point. (c) The transition point is zoomed-in yet more to show the details of the behavior.

Figure 8: (a)  $F_v$  vs.  $t$  for the same case of the  $A = 100$  statvolt,  $\phi = \pi/4$  CP wave acting on the spiraling classical electron, as occurs in Fig. 7. This plot corresponds with the same time period as shown for the  $r$  vs.  $t$  curve in Fig. 7(c). (b)  $r$  vs.  $t$  and  $F_v$  vs.  $t$ , zoomed in to the point near  $t = 3.2 \times 10^{-12}$  sec, where the transition of spiraling decay sets in. (c)  $r$  vs.  $t$  and  $F_v$  vs.  $t$ , for the same trajectory of this  $A = 100$  statvolt,  $\phi = \pi/4$  case, but near  $t = 0$ .

Figure 9: (a) Four curves of  $r$  vs.  $t$  are shown, one with  $A = 0$ , and three involving a single CP plane wave of  $A = 100$  statvolts acting on the orbiting particle, but with phases  $\phi = \frac{1}{4}\pi$ ,  $\frac{3}{8}\pi$ , and  $\frac{1}{2}\pi$  between  $\mathbf{E}$  and the initial velocity  $\dot{\mathbf{z}}$ . (b) The initial region of Fig. 9(a), near  $t = 0$ , is zoomed in on here, to show how the  $A = 0$  and  $A = 100$  statvolt,  $\phi = \pi/2$  curves correspond. (c) Here the  $\phi = \frac{1}{4}\pi$  curve in Fig. 9(a) is superimposed over the  $\phi = \frac{3}{8}\pi$  curve, by translating the two curves in time (not changing shapes, just displacing in time) so that the first hump on the right to the transition point line up. As can be seen, after this displacement, the two curves are nearly indistinguishable.

Figure 10: (a)  $r$  vs.  $t$ , where the electron is started in a circular orbit from three different radii ( $r = 0.515 \text{ \AA}$ ,  $0.525 \text{ \AA}$ , and  $0.535 \text{ \AA}$ ), and where in each case the same CP plane wave acts, with  $A = 100$  statvolt,  $\phi = 0$ , and with a frequency equal to the orbital frequency of the electron in a circular orbit of radius  $0.5 \text{ \AA}$ . Also shown are three other curves, with the same orbital starting conditions, but with  $A = 0$ . (b) Here the center curve in Fig. 10(a) is zoomed in on to reveal the resonance-like behavior that occurs when the electron gets near the  $r = 0.5 \text{ \AA}$ .

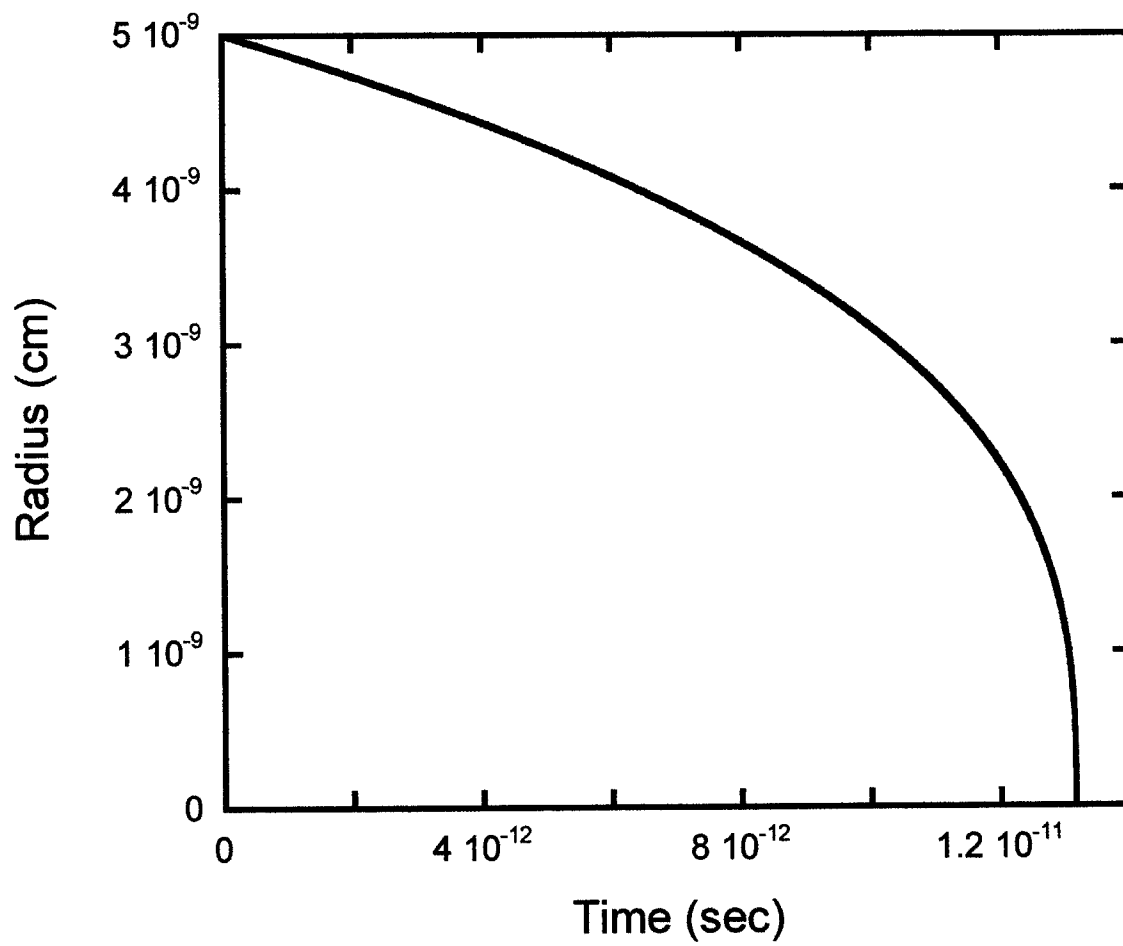


Fig. 1

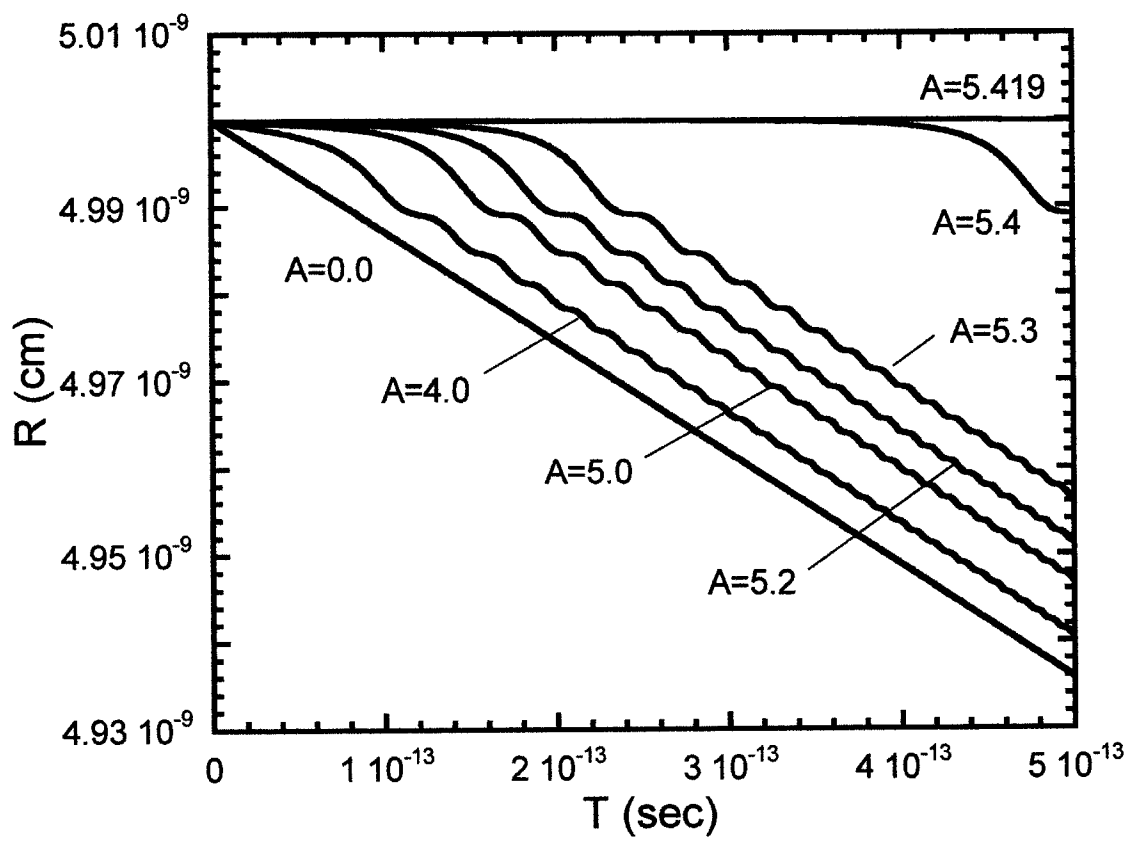


Fig 2

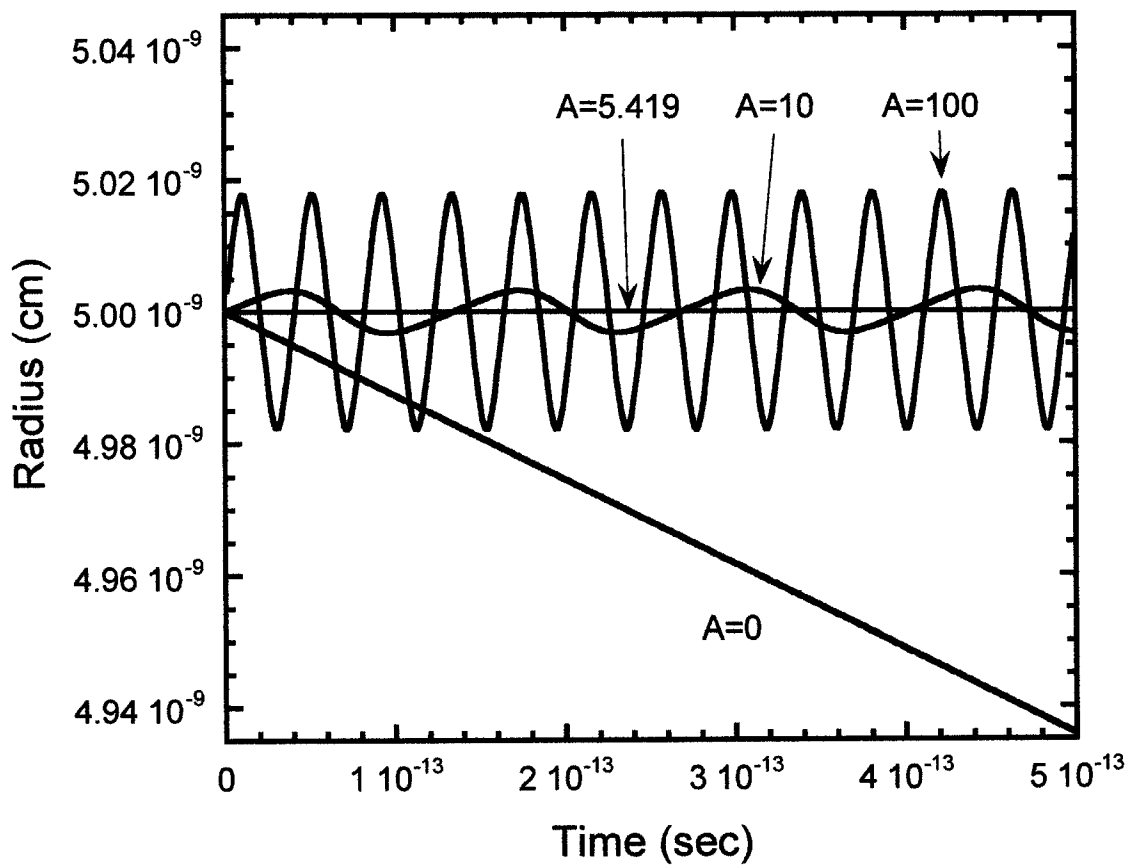


Fig 3a

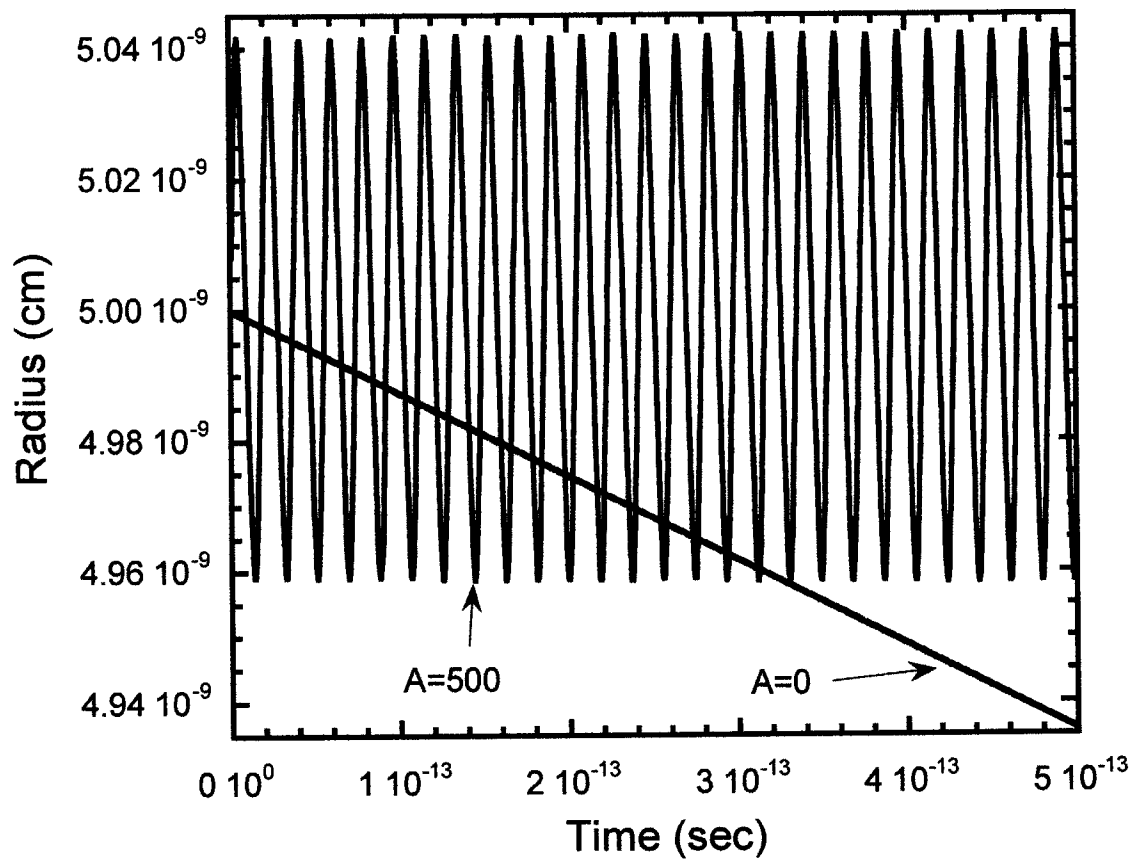


Fig. 3b

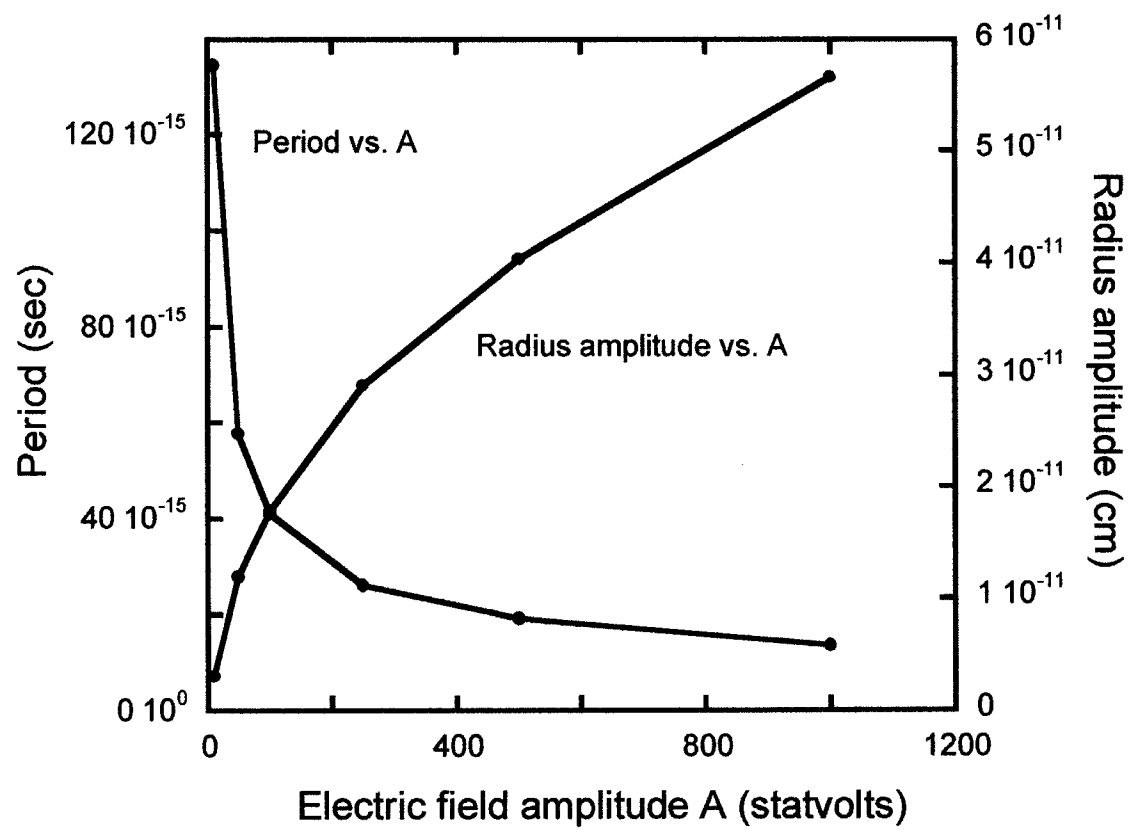


Fig. 4

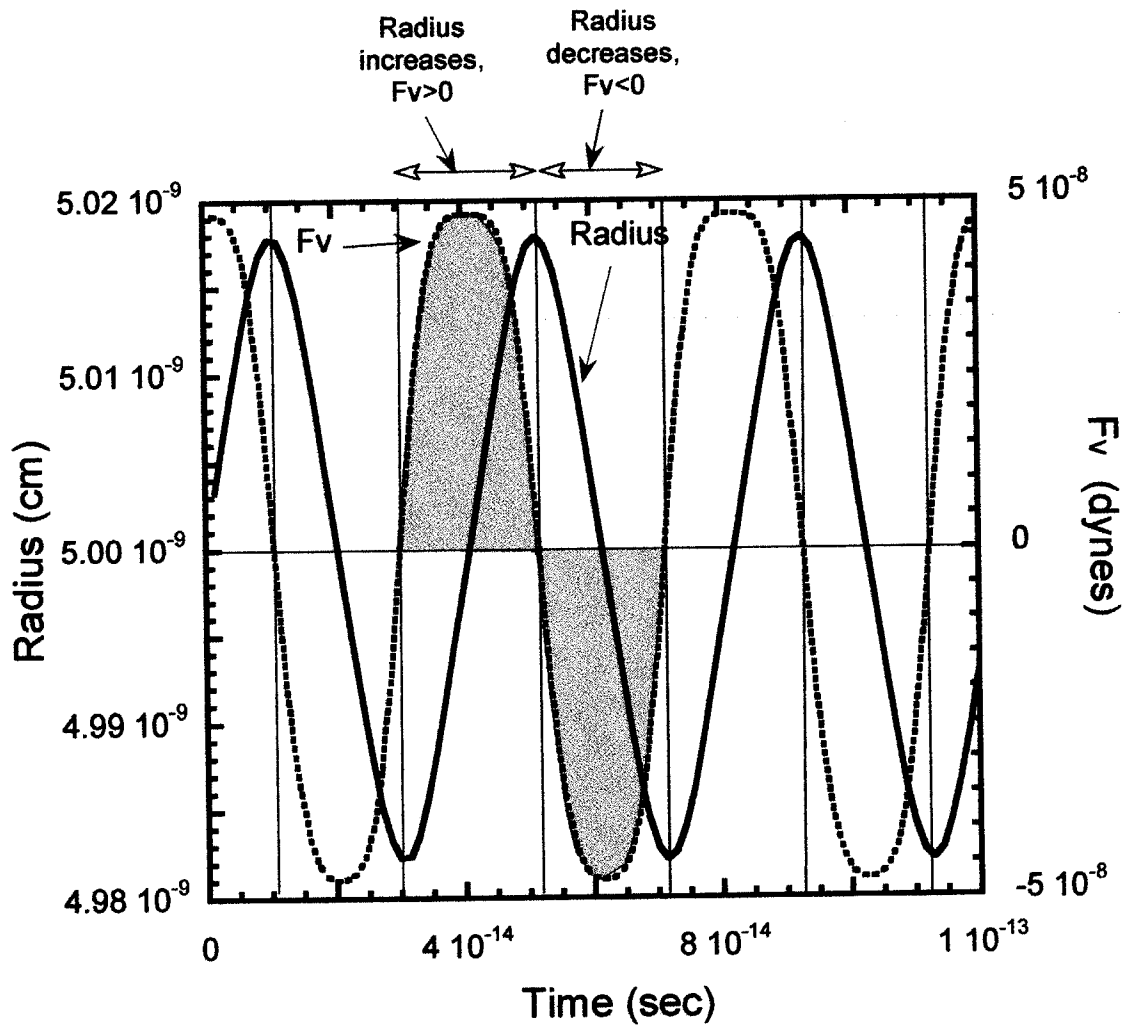


Fig. 5



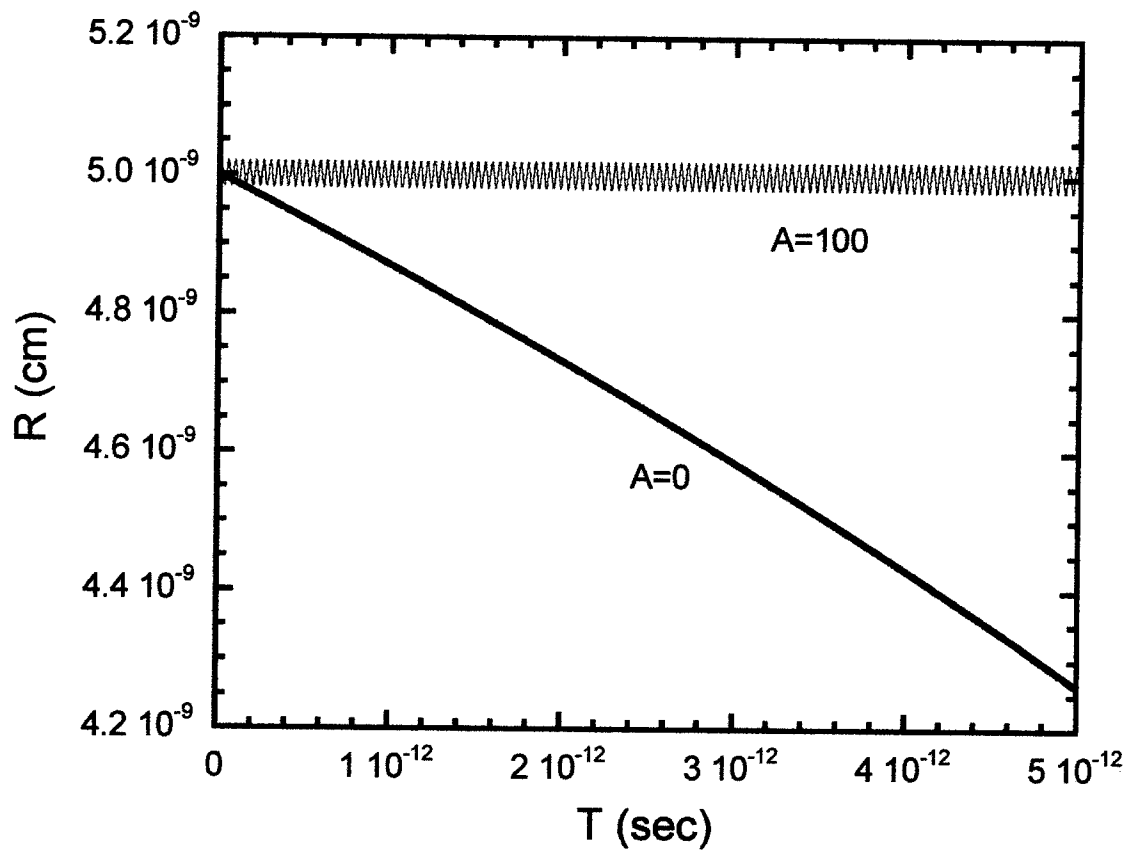


Fig. 6a

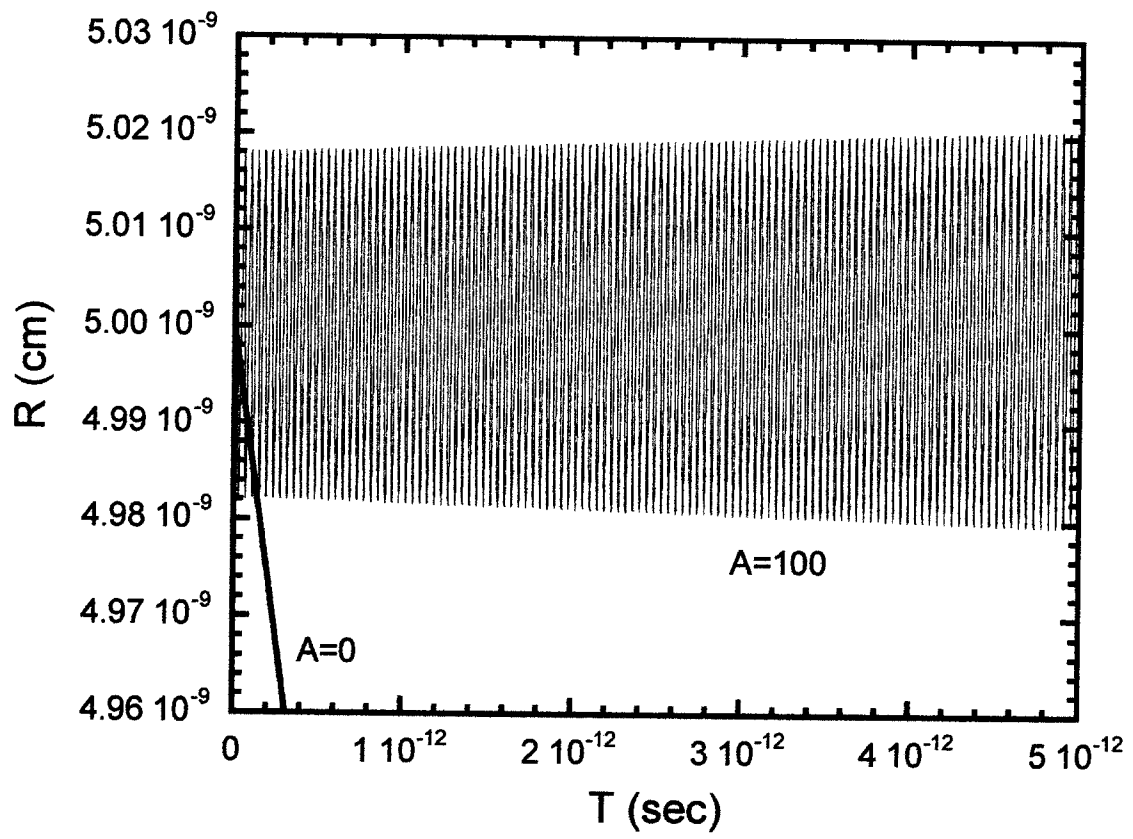


Fig. 6b

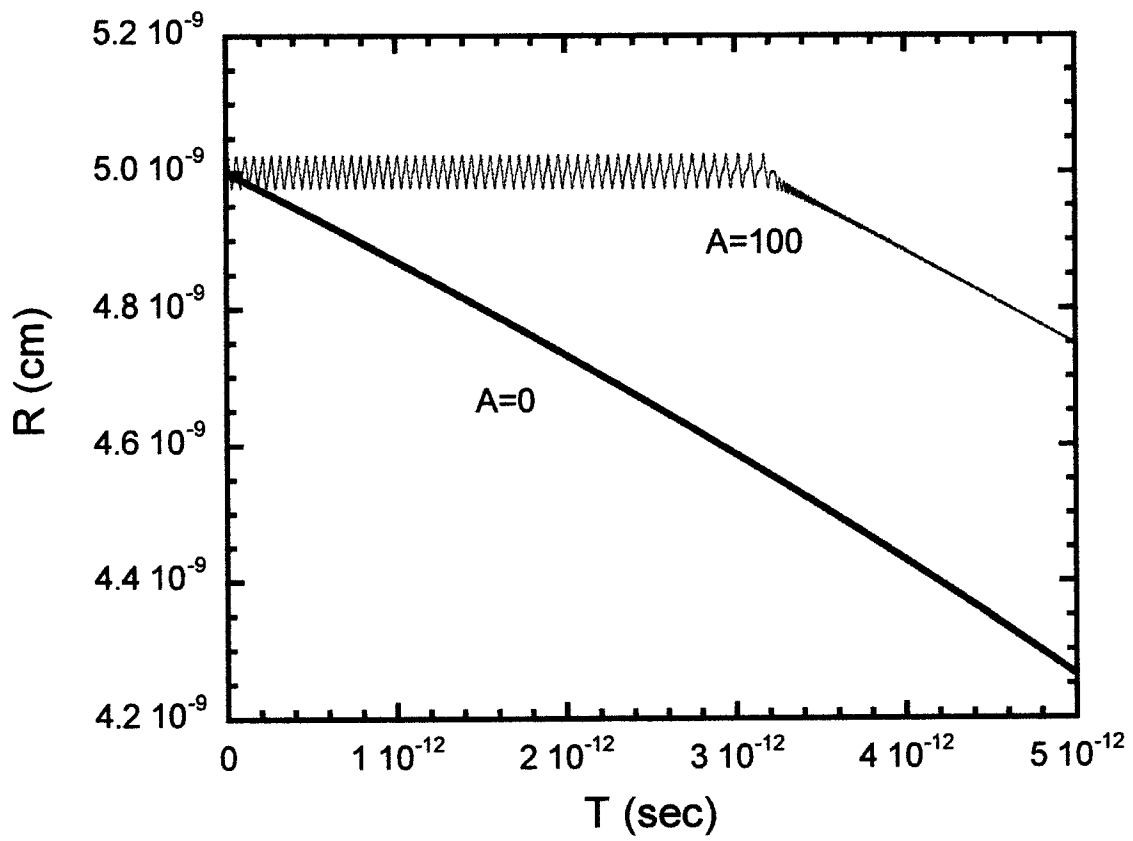


Fig. 7a

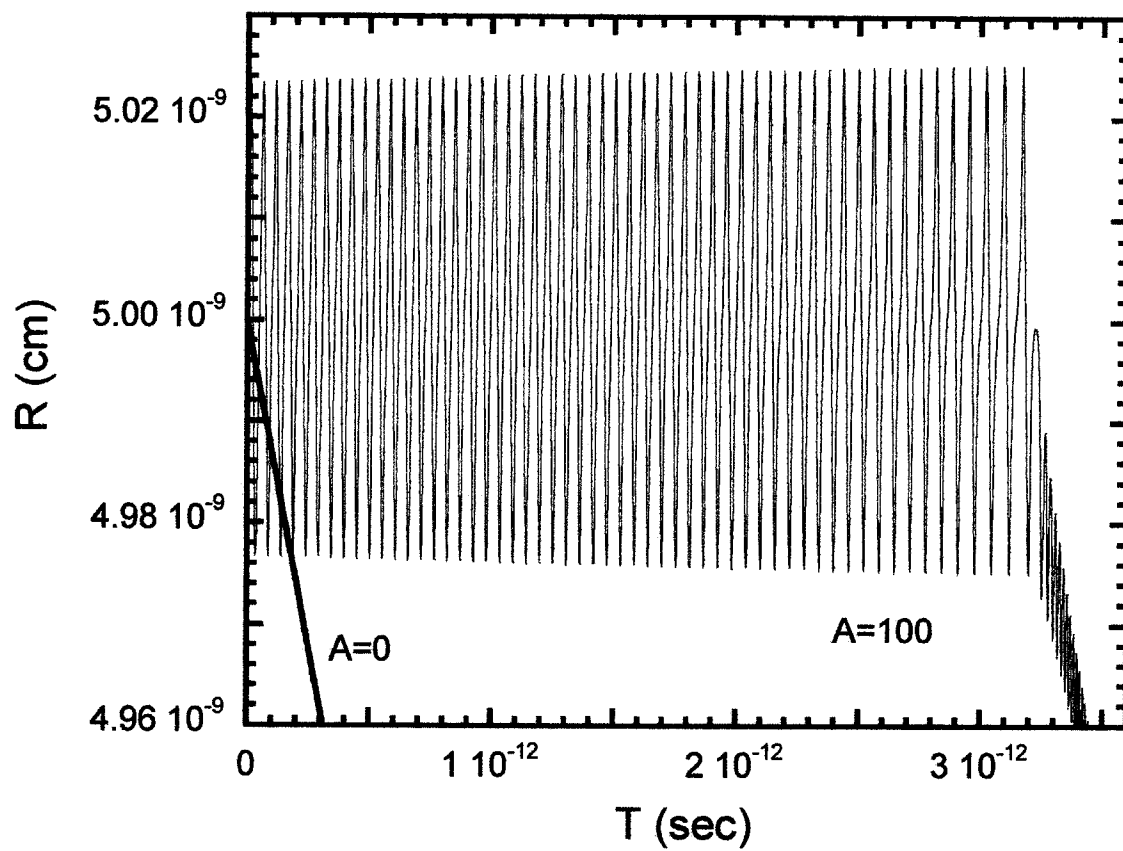


Fig. 7b

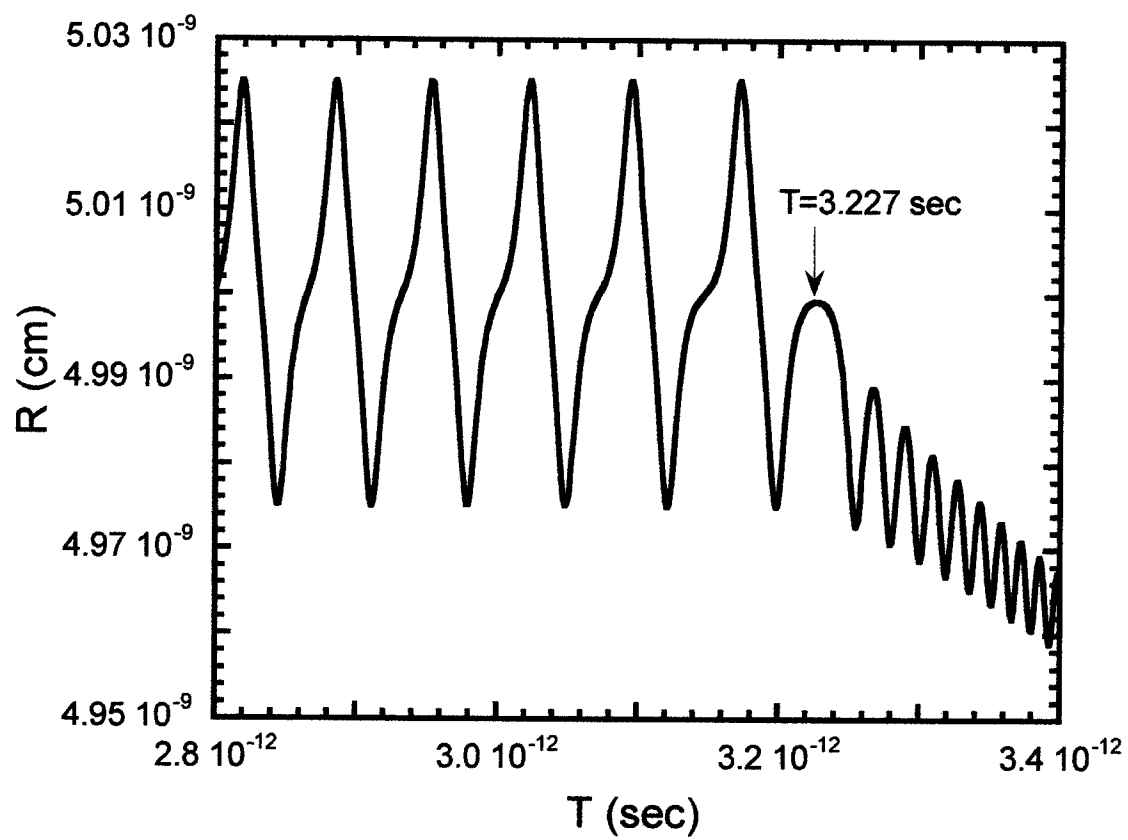


Fig. 7c

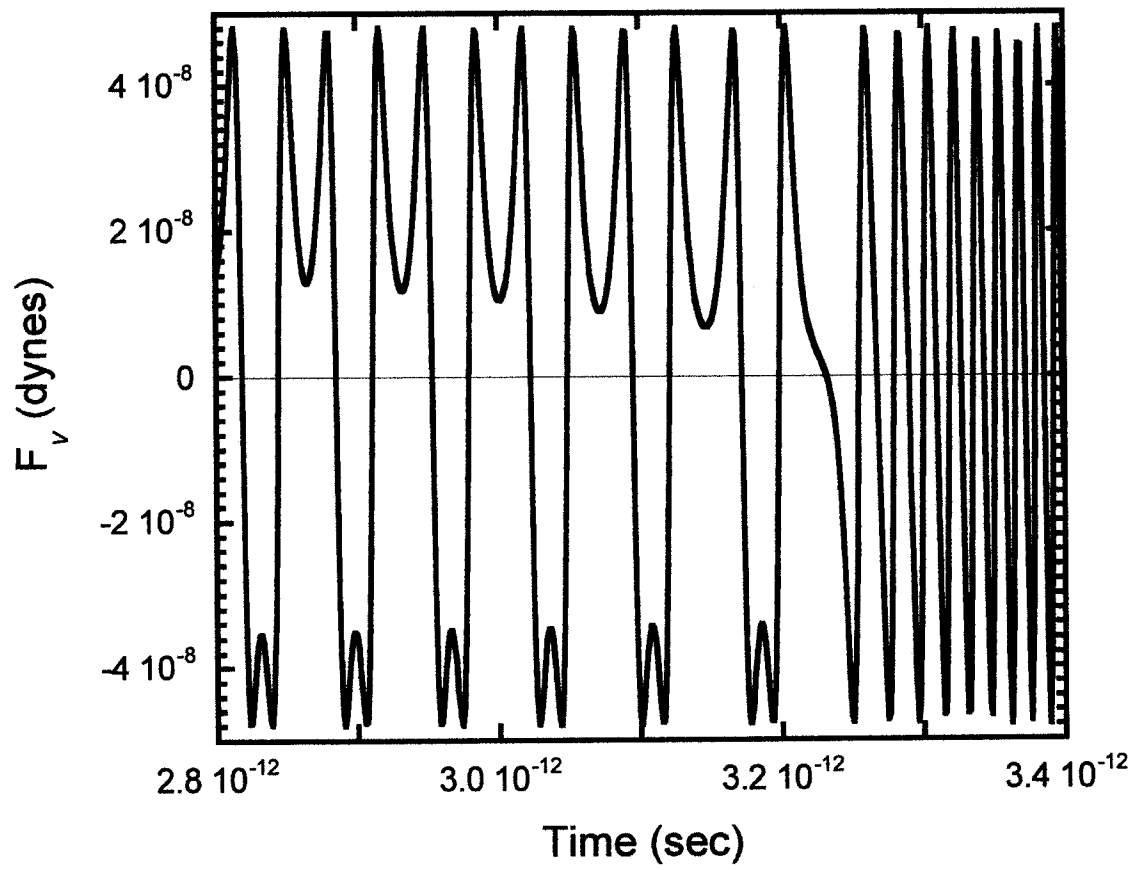


Fig. 8a

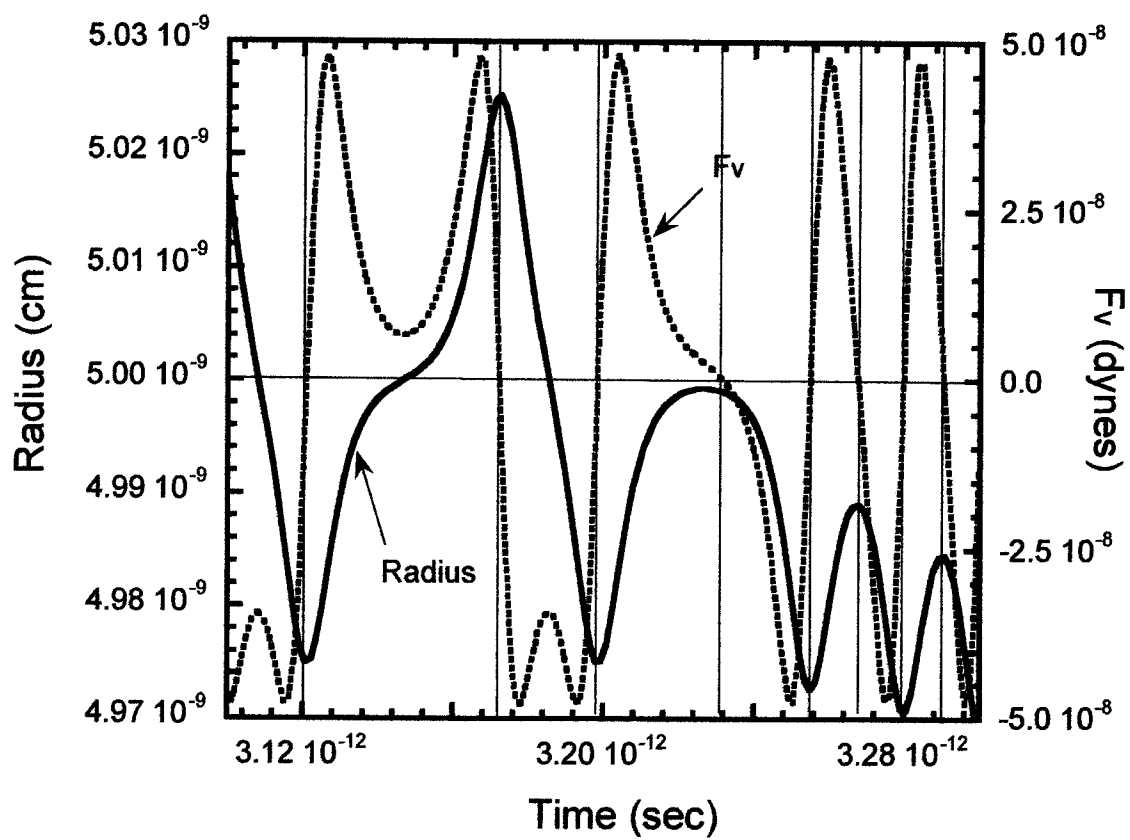


Fig. 8b

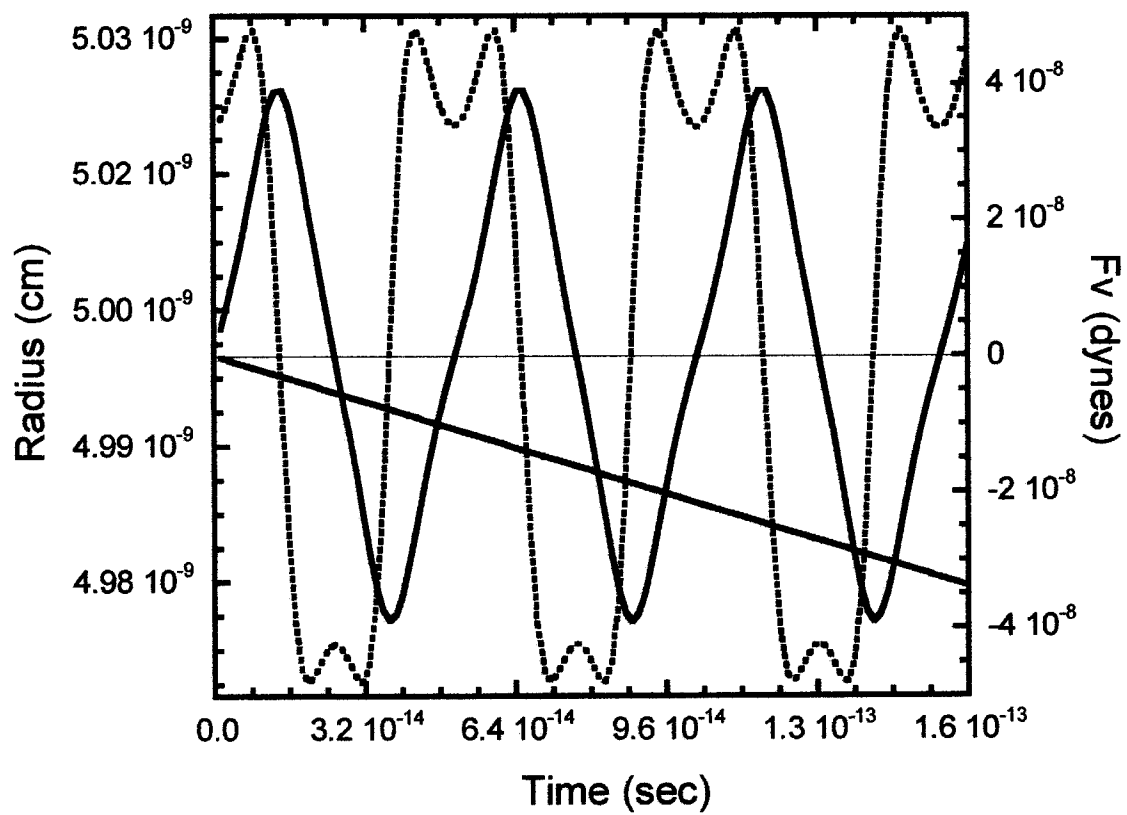
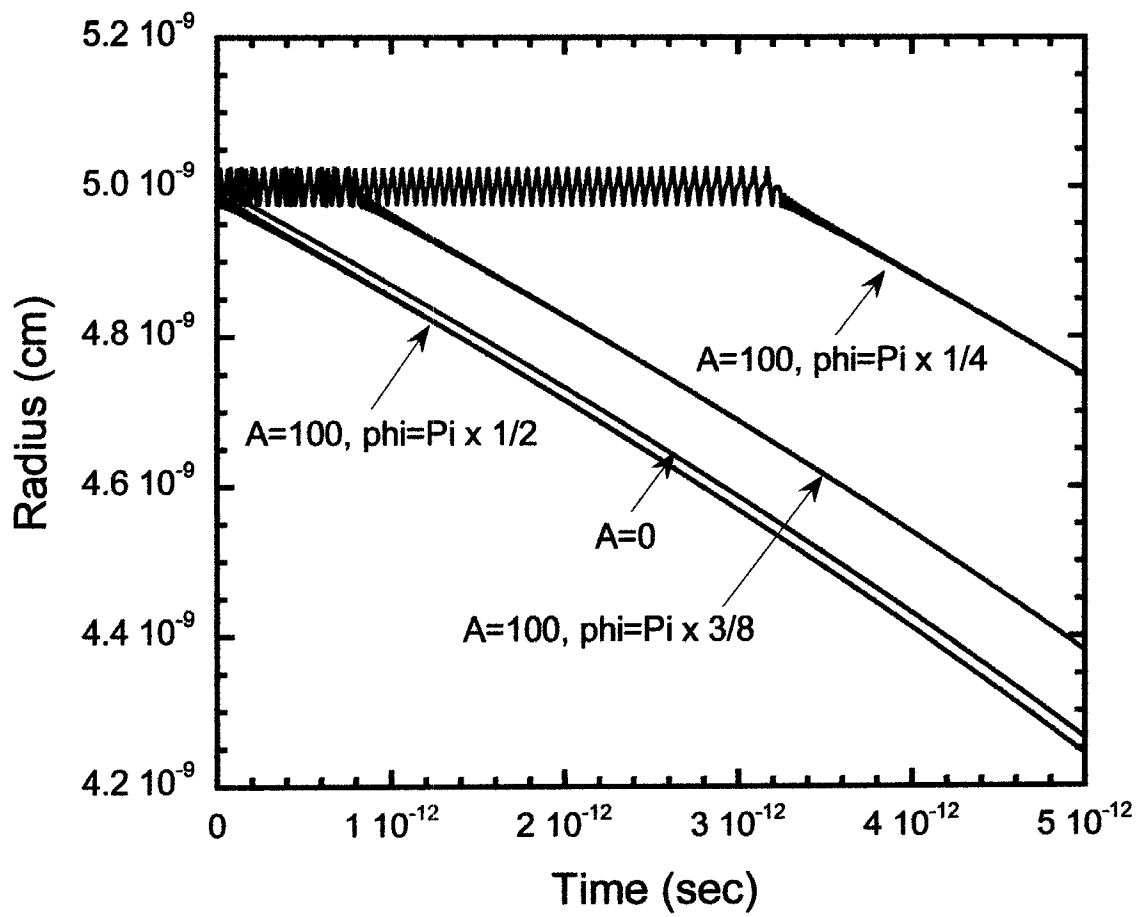


Fig. 8c





**Fig 9a**

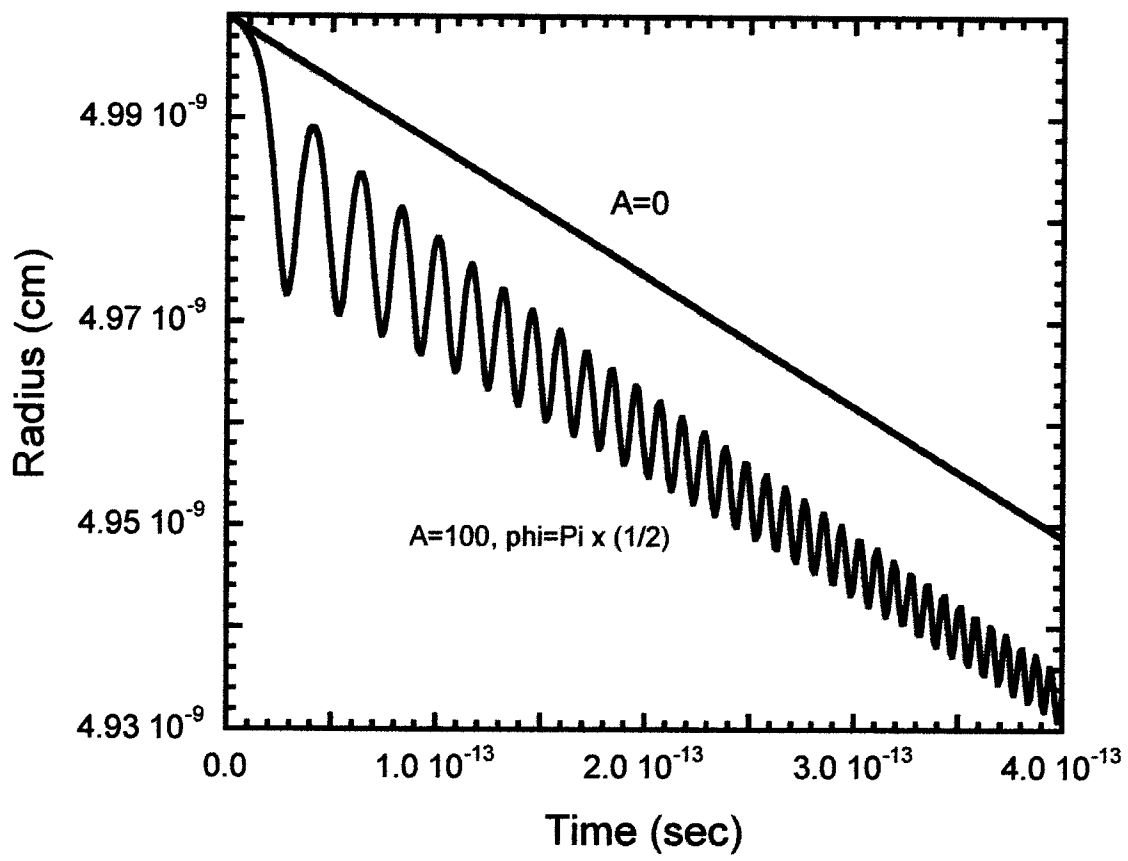


Fig. 9b

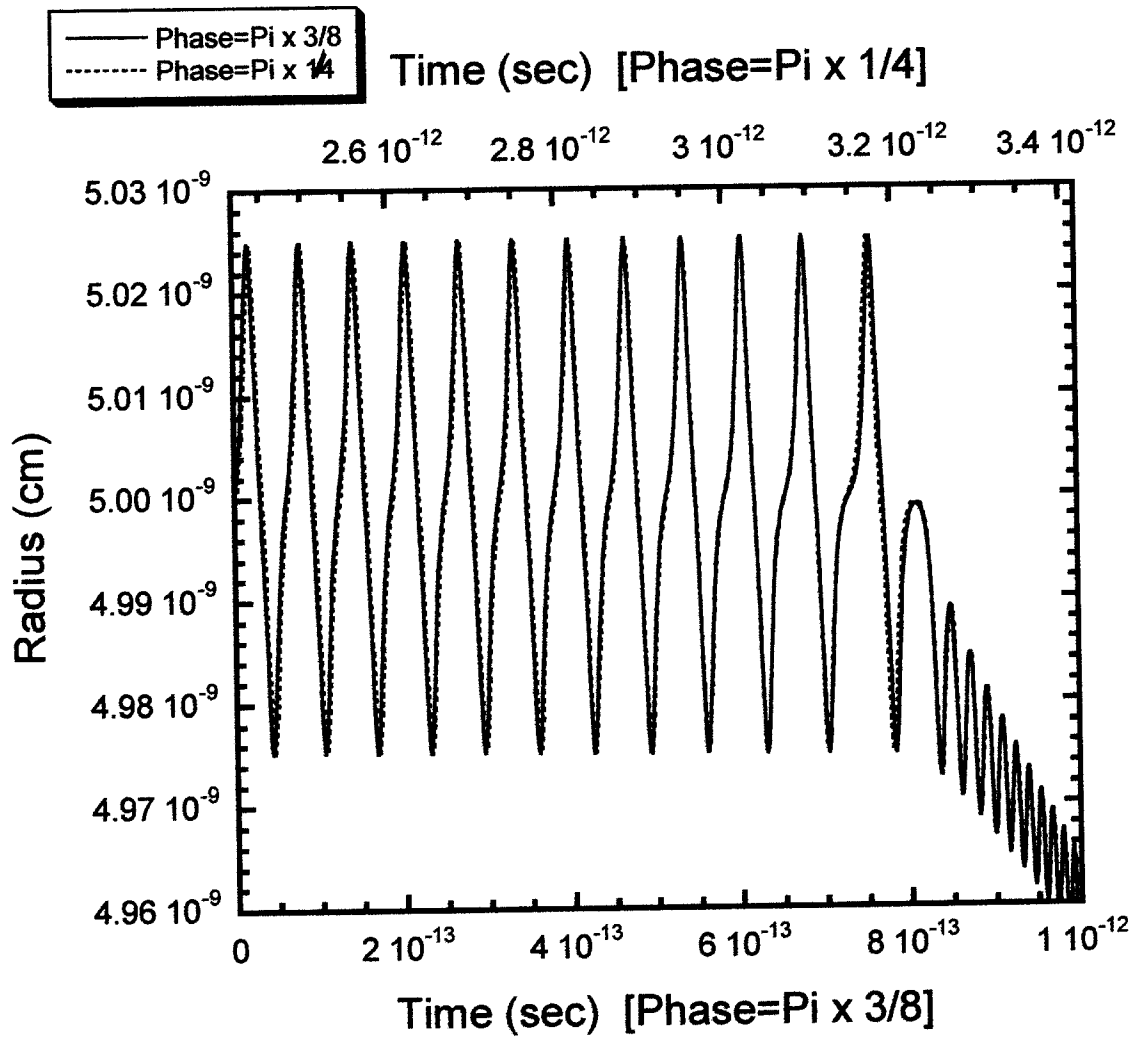


Fig. 9c

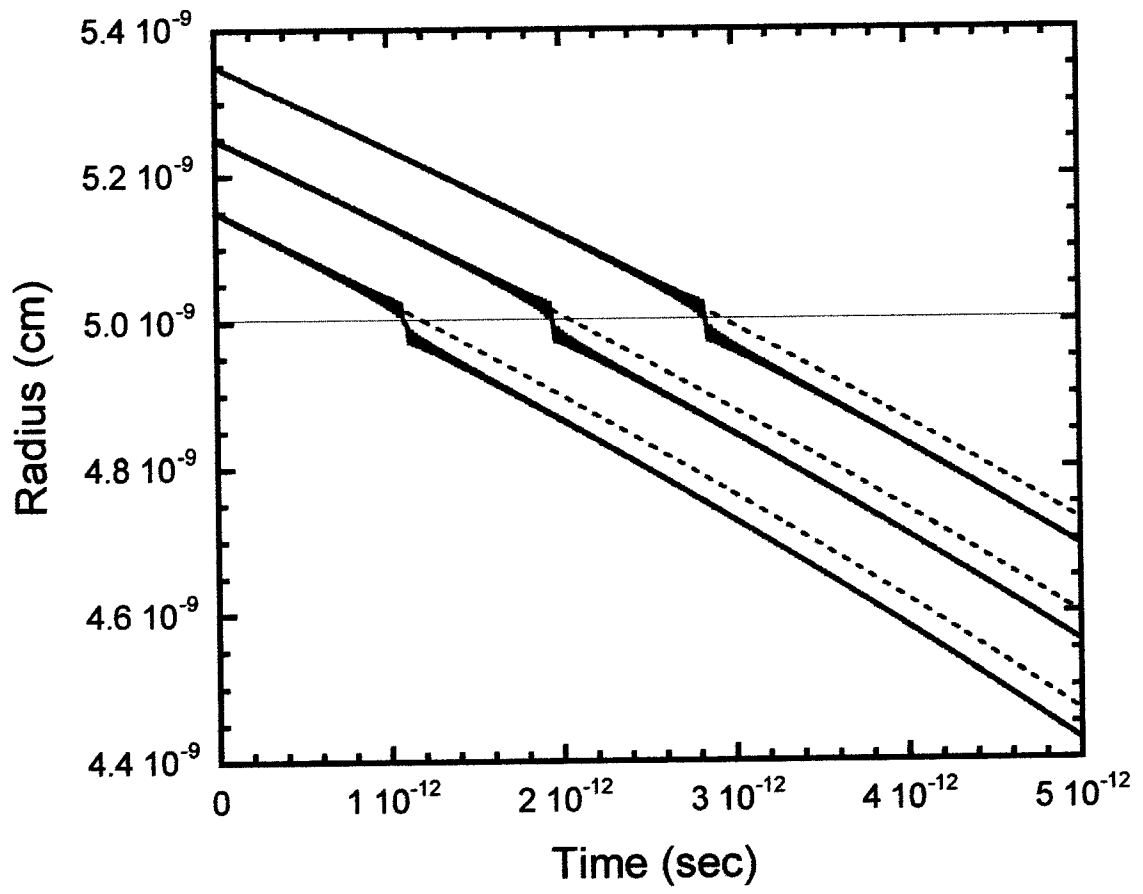


Fig. 10a

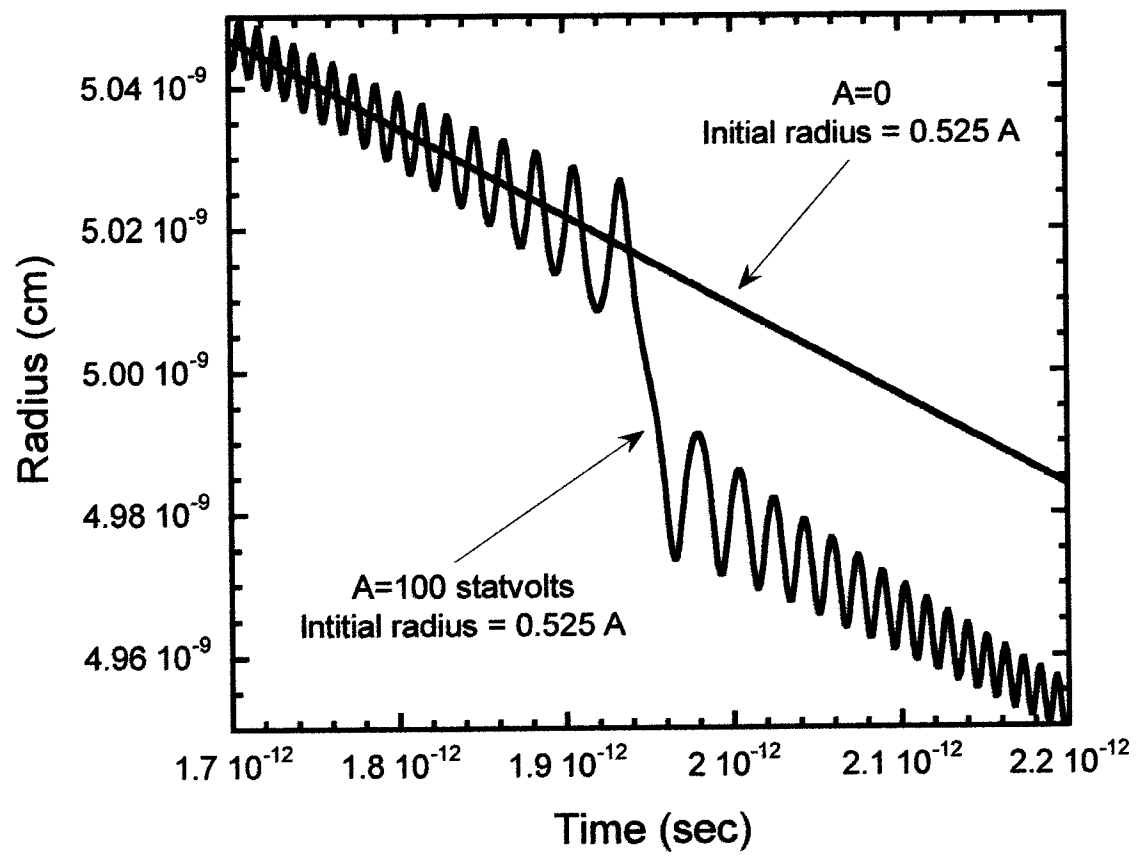


Fig. 10b